UNIVERSIDAD DE CHILE
FACULTAD DE CIENCIAS FÍSICAS Y MATEMÁTICAS
DEPARTAMENTO DE INGENIERÍA CIVIL

DESARROLLO E IMPLEMENTACIÓN DE UN MODELO PARA EL ESTUDIO DE LA DINÁMICA A LARGO PLAZO DEL DIÓXIDO DE CARBONO Y OXÍGENO EN EL SALAR DE HUASCO, CHILE

TESIS PARA OPTAR AL GRADO DE MAGÍSTER EN CIENCIAS DE LA INGENIERÍA, MENCIÓN RECURSOS Y MEDIO AMBIENTE HÍDRICO

MEMORIA PARA OPTAR AL TÍTULO DE INGENIERA CIVIL

KARINA MARCELA VALENZUELA MARTÍNEZ

PROFESORA GUÍA:
ANA LUCÍA PRIETO SANTA

MIEMBROS DE LA COMISIÓN:
ALBERTO DE LA FUENTE STRANGER
FRANCISCO SUÁREZ POCH

Este trabajo ha sido parcialmente financiado por Fondecyt Regular N° 1221191

SANTIAGO DE CHILE
2024

RESUMEN DE LA TESIS PARA OPTAR AL GRADO DE: Magíster en Ciencias de la Ingeniería, mención Recursos y Medio Ambiente Hídrico
MEMORIA PARA OPTAR AL TÍTULO DE: Ingeniera Civil
POR: Karina Marcela Valenzuela Martínez
FECHA: 2024
PROFESORA GUÍA: Ana Lucía Prieto Santa

DESARROLLO E IMPLEMENTACIÓN DE UN MODELO PARA EL ESTUDIO DE LA DINÁMICA A LARGO PLAZO DEL DIÓXIDO DE CARBONO Y OXÍGENO EN EL SALAR DE HUASCO, CHILE

Los salares altiplánicos son oasis que sustentan la vida en cuencas endorreicas de Sudamérica. Estos sistemas se caracterizan por presentar condiciones ambientales extremas y un gran valor ecológico. Sin embargo, se encuentran amenazados debido a que albergan yacimientos de diferentes minerales cuya extracción impacta en las fuentes de agua superficial y subterránea. Sumado a esto, el cambio climático podría modificar las condiciones de estos ambientes, desequilibrando ciclos del agua y procesos bioquímicos. La actividad microbiana presente en los lagos salinos desempeña un papel clave en el reciclaje de gases de efecto invernadero. Estas comunidades pueden verse afectadas debido a la influencia de factores atmosféricos sobre los procesos que ocurren en estos sistemas. Para poder analizar estos efectos se construye un modelo 0-D impermanente mediante la utilización de herramientas computacionales (Matlab y Python) que permite simular a largo plazo (1948 a 2021) los flujos de masa a través de interfaces (aire-agua y agua-sedimento) y los procesos bioquímicos (fotosíntesis, fotorrespiración, respiración, demanda biológica de oxígeno e incremento/decaimiento de concentración de biomasa y detritos) relacionados con las concentraciones de CO_2 y O_2 en la laguna del Salar de Huasco, el cual corresponde a un área silvestre protegida ubicada en el norte de Chile. Este trabajo tiene como objetivo estudiar la influencia de las tendencias climáticas de factores meteorológicos en lagos salinos de gran altitud y su relación con la dinámica del CO_2 y O_2. El modelo permite estudiar el comportamiento de las variables de control durante un período de más de 70 años y a diferentes escalas temporales. Esta perspectiva a largo plazo logra alcanzar un estado donde los equilibrios y ciclos que caracterizan la respuesta del sistema son independientes de las condiciones iniciales. Los resultados indican que los transportes de masa a través de la interfaz aire-agua son procesos clave en la variación de las concentraciones de CO_2 y O_2. Se demostró que las variables atmosféricas influyen en el transporte de masas y en la calidad de agua de los lagos salinos de gran altitud, siendo la velocidad del viento el factor más significativo. Es importante señalar que cuando se habla de cambio climático se suele hacer hincapié en las fluctuaciones de la temperatura ambiental; sin embargo, en este trabajo se demuestra que un factor relevante a considerar es la variación del régimen de vientos.

Agradecimientos

El camino para llegar hasta aquí fue muy largo y dentro de toda esta etapa existieron muchas personas que fueron un gran apoyo y que me dieron la energía necesaria para seguir esforzándome y lograr cumplir mis objetivos ✦.

En primer lugar, quiero agradecer a mis hermanos, mis cuñadas, mis sobrinos, mi madrina y especialmente a mis padres: Vivi y Juanca, que en todo momento me han dado las fuerzas para seguir creciendo y me han entregado todo su apoyo en las decisiones que he tomado. Gracias por estar presentes y por motivarme a enfrentar nuevos desafíos, siempre diciéndome que podría resolver y solucionar cualquier situación que enfrentara ♡.

Estoy infinitamente agradecida de mi pareja, compañero y mejor amigo: Alan. Agradezco todas las palabras de aliento que me entregaste durante todo este proceso. Gracias por darme muchos ánimos, apoyarme en cada decisión y creer en mí más que yo misma. Fuiste un pilar fundamental en el desarrollo de mi tesis, sabías qué decir en cada momento de estrés y me ayudaste a confiar más en mis capacidades. Te amo ♥.

También quiero agradecer a mis amigas del colegio, a mis compañeros/as de Bachi y a todos los que conocí en Beauchef. En particular, muchas gracias a Stefi, Vale y Cata por cada junta de estudio, almuerzo, salida, carrete, etc. Gracias por llenar mi etapa universitaria de miles de momentos inolvidables. Muchas gracias a la gente de la salita de tesistas, en especial a Naro, Montse y Gabi por todo el apañe en mi paso por el magíster. Se agradece cada completada bailable, celebración de 18 y amigo secreto/robado realizado en el 3er piso. También agradecer a Jacqui por la disponibilidad y la paciencia de explicar y dar solución a cualquier duda ❀.

Muchas gracias a las chicas de balonmano y a Seba; ustedes me enseñaron a trabajar en equipo, a no rendirse y a luchar por tus metas hasta el final, ya que todo esfuerzo tiene sus recompensas. Gracias por los 5 años de entrenamientos, triunfos, derrotas y por sobre todo aprendizaje 🏆.

Quiero agradecer a los profesores que me dieron la oportunidad de desarrollar esta tesis: profe Ana y profe Beto. Gracias por confiar en mí, por entregarme tanto conocimiento, por ayudarme en cada etapa y darme todas las herramientas necesarias para realizar este gran trabajo ☆.

Gracias a mis compañeros perrunos que siempre han estado a mi lado, acompañándome y subiéndome el ánimo. Los amo infinito Lupita y Betito 🐾.

Por último y no menos importante, quiero agradecerme a mí misma por no rendirme a pesar de lo difícil que se volvió el proceso en varias ocasiones. Gracias por querer seguir aprendiendo, por darlo todo y por atreverte a enfrentar los diferentes obstáculos y desafíos ✿.

¡Muchas gracias a tod@s!

Tabla de Contenido

I. Introducción

Los salares de altura se caracterizan por condiciones ambientales extremas con baja presión parcial de O_2, alta radiación, oscilaciones térmicas intradiarias extremas y condiciones de agua dulce a hipersalina (Dorador et al., 2020; Hernández et al., 2016). Estos sistemas presentan costras de sal que rodean los lagos salinos, cuyo suministro de agua proviene principalmente de flujos subterráneos (de la Fuente et al., 2021; Marazuela et al., 2019). Aunque se pueden encontrar lagos salinos en todos los continentes, los lagos salinos de gran altitud se encuentran principalmente en la meseta del Tíbet y en las tierras altas de América del Sur (Finlayson, 2018). En Sudamérica, existen lagos salinos por sobre los 3000 msnm ubicados en depresiones centrales de cuencas endorreicas en zonas altiplánicas de Chile, Bolivia, Perú y Argentina (de la Fuente et al., 2021; Suárez et al., 2020).

Estos ecosistemas dinámicos se caracterizan por la presencia de comunidades microbianas que realizan un intenso reciclaje de nutrientes, los cuales limitan la producción primaria bruta (PPB) (Gao et al., 2021; Huang et al., 2023; Yue et al., 2021). En la base trófica, las diatomeas y las cianobacterias gobiernan los flujos de dióxido de carbono y oxígeno en el lago (de la Fuente, 2014; Dorador et al., 2020; Paquis et al., 2023). Los lagos salinos tienen un gran valor ecológico, ya que son oasis que albergan una gran variedad de especies que tienen mecanismos fisiológicos y bioquímicos que les permiten tolerar las condiciones extremas de las regiones áridas, pero son muy sensibles incluso a pequeños cambios en el clima (Finlayson, 2018). Sin embargo, estos sistemas acuáticos están amenazados por una mayor demanda de minerales de alto valor (por ejemplo, litio), lo que implica un aumento en las extracciones de agua subterránea (Halkes et al., 2024; Marazuela et al., 2019). En el caso de las lagunas hipersalinas (>40 $\frac{g}{L}$), estas son consideradas laboratorios naturales con un valor científico único porque albergan una biodiversidad reducida con redes tróficas simples en comparación con otros sistemas acuáticos; por lo tanto, son extremadamente sensibles al bombeo de salmuera y/o agua (Gajardo y Redón, 2019).

Los lagos salinos pueden desempeñar un papel vital en el contexto del cambio climático, ya que la actividad microbiana presente en estos sistemas puede contribuir al reciclaje de gases de efecto invernadero (GEI) a través de diferentes procesos (por ejemplo, fijación del carbono, nitrificación y metanogénesis), actuando como sumideros o fuentes de estos gases (Molina et al., 2018; Veihelmann et al., 2023). Sumado a esto, el cambio climático podría modificar las condiciones físicas de estos ambientes, desequilibrando el ciclo local del agua y los procesos bioquímicos naturales (Uribe Rivera et al., 2017). Según Wurtsbaugh et al. (2017), el aumento de las temperaturas y las variaciones en la evaporación y precipitación pueden hacer que los límites de salinidad aumenten más allá de la tolerancia de invertebrados como el camarón de salmuera (*Artemia spp*.) y las moscas de salmuera (*Ephedra spp*.) que forman parte de la base alimenticia de las aves, especialmente de los flamencos. Además, la desecación de los lagos da lugar a la formación de extensas fuentes de polvo fino que pueden ser una amenaza para la salud humana (Wurtsbaugh et al., 2017).

Los estudios de monitoreo in situ permiten comprender cómo los forzamientos meteorológicos afectan la dinámica de los nutrientes, el dióxido de carbono y el oxígeno en sistemas complejos y extremos, como los lagos salinos de gran altitud. La campaña de campo E-DATA (Evaporation caused by Dry Air Transport over the Atacama Desert) de noviembre del 2018 se llevó a cabo en el Salar de Huasco y permitió investigar la relación entre las condiciones meteorológicas y la dinámica bioquímica en las aguas abiertas del lago salino (Suárez et al. 2020). Suárez et al. analizaron los efectos del viento sobre el flujo de CO_2 a través de la interfase aire-agua y encontraron que existe una fuerte correlación entre los regímenes de viento, la evaporación y los procesos bioquímicos presentes en el Salar de Huasco, enfatizando que el cambio climático puede afectar los patrones de viento. Por otro lado, de la Fuente (2014) menciona que existen ciclos meteorológicos diurnos donde el viento impacta los mecanismos de transferencia de calor y masa entre el lago del Salar de Huasco y la atmósfera. Por ejemplo, durante las noches y mañanas la superficie del agua se caracteriza por condiciones de calma y baja resuspensión de sedimentos. Durante la tarde dominan condiciones ventosas que promueven la resuspensión de sedimentos y los intercambios entre la interfase aire-agua (AWI) y la interfase agua-sedimento (WSI) (de la Fuente, 2014). El ciclo estacional que caracteriza la precipitación en el Altiplano está dominado por cambios en el flujo zonal, donde los vientos del este favorecen condiciones húmedas (verano) y los vientos del oeste provocan condiciones secas (invierno) (Garreaud et al., 2003). Otros estudios han indicado que la circulación atmosférica es un factor dominante que controla los flujos superficiales en el desierto (por ejemplo, la evaporación) y descarta a la energía asociada a la radiación como principal factor limitante (Aguirre-Correa et al., 2023; Lobos-Roco et al., 2021).

Como se ha mencionado anteriormente, los microorganismos desempeñan un papel clave en el reciclaje de GEI e influyen en el equilibrio de materia orgánica y energía en los lagos salinos. La magnitud, el flujo y la dirección (fuente o sumidero) de los GEI en lagos salinos tienen una dinámica temporal que se ve afectada por cambios estacionales relacionados con la temperatura, la radiación, el viento y el agua disponible, que generan variaciones en las comunidades microbianas (Dorador et al., 2020; Molina et al., 2021). Existe una compleja interacción entre los factores ambientales y la calidad y dinámica del agua en los lagos salinos. Por ejemplo, en dos lagos salinos poco profundos (Lago Los Flamencos en Chile y Lago Khalina en Bolivia) se encontraron relaciones entre las fluctuaciones estacionales de temperatura y variables de calidad del agua como salinidad, turbidez y concentración de biomasa de fitoplancton (De los Rios-Escalante et al., 2024). Otro estudio en el Salar del Huasco indica que el rol activo de las comunidades microbianas puede verse afectado por la estacionalidad (períodos húmedos y secos) que genera alteraciones en las condiciones físicas y químicas del agua, provocando un desequilibrio en el ecosistema (Paquis et al., 2023).

Aunque los estudios a corto plazo han proporcionado valiosos conocimientos sobre los lagos salinos, especialmente a escala intradiaria, es imprescindible profundizar en el comportamiento a largo plazo de estos sistemas, ya que los factores ambientales que influyen en los flujos verticales, la actividad microbiana y el secuestro/almacenamiento de GEI pueden variar al pasar a escalas estacionales o anuales (Molina et al., 2021; Pardo-Esté et al., 2023; Richardson et al., 2024). La

modelación computacional se convierte en una herramienta esencial para comprender el comportamiento de estos sistemas complejos, teniendo en cuenta que el monitoreo de los diferentes procesos en lugares extremos, como los lagos salinos de gran altitud, y la predicción de sus efectos debido al cambio climático no siempre son factibles. La perspectiva a largo plazo permite alcanzar un estado en el que los equilibrios y ciclos que caracterizan la respuesta del sistema son independientes de las condiciones iniciales.

I.I Objetivo

Este trabajo pretende estudiar la influencia de las tendencias climáticas de variables meteorológicas en lagos salinos de gran altitud y su relación con el mecanismo que gobierna las concentraciones de CO_2 y O_2 en la columna de agua. Se presta especial interés al transporte de CO_2 y O_2 a través de las interfases aire-agua y agua-sedimento, a los procesos de consumo/producción relacionados con la producción primaria y a los efectos de las forzantes meteorológicas sobre la calidad del agua. Para esto se construye un modelo 0-dimensional impermanente con el fin de analizar los flujos y concentraciones de CO_2 y O_2 en la laguna del Salar de Huasco a largo plazo (1948-2021) y estudiar la dinámica de estas variables a diferentes escalas temporales. Para desarrollar este modelo se utilizan datos meteorológicos y de calidad de agua medidos en dos campañas de terreno (mayo del 2016 y noviembre del 2018), junto con los resultados que entrega un estudio realizado por de la Fuente y Meruane (2017) donde elaboran un modelo espectral que entrega simulaciones a largo plazo en humedales someros. El presente trabajo proporciona una herramienta valiosa para investigadores que buscan comprender los efectos de los factores ambientales relacionados con el cambio climático en los sistemas acuáticos.

II. Artículo para publicación

Modeling long-term dynamics of carbon dioxide and oxygen in high-altitude saline lakes

Karina Valenzuela[1], Ana L Prieto[1,2], Francisco Suárez[3] and Alberto De la Fuente[1*]
[1]Departamento de Ingeniería Civil, Universidad de Chile, Santiago, Chile
[2]Centro Avanzado para Tecnologías del Agua, CAPTA, Universidad de Chile, Santiago, Chile
[3]Departamento de Ingeniería Hidráulica y Ambiental, Pontificia Universidad Católica de Chile, Santiago, Chile
*Corresponding author. aldelafu@ing.uchile.cl

Keywords: Salar del Huasco; high-altitude saline lakes; multiscale processes; CO_2 and O_2 dynamics; interface fluxes; atmospheric forcings

Abstract

Altiplanic saline lakes are located above 3000 m.a.s.l. in endorheic basins in South America. Extreme environmental conditions and great ecological value characterize these systems. However, they are threatened because they host great mineralogical wealth. In addition, climate change could impact these environments, unbalancing water cycles and biochemical processes. Saline lakes play a key role in recycling greenhouse gases through microbial activity, which can alter the effects of meteorological forcings. To analyze these effects, we constructed a transient 0-D model that simulates interphase mass fluxes and biochemical processes related to CO_2 and O_2 in the Salar del Huasco lagoon, corresponding to a protected wilderness area in northern Chile. This article aims to study the influence of climatic trends of meteorological variables in high-altitude saline lakes and their relationship with CO_2 and O_2 dynamics. The model allows studying the long-term behavior of control variables independent of initial conditions and at different time scales. The results indicate that mass transport of CO_2 and O_2 across the air-water interface dominates variations of the concentrations in the column water. Atmospheric forcings were shown to influence mass transport and water quality in high-altitude saline lakes, with wind speed being the most significant factor. It is important to note that when talking about climate change, emphasis is usually placed on fluctuations in ambient temperature; however, it is shown that it is relevant to consider the variation of the wind regime.

1. Introduction

High-altitude salars are characterized by extreme environmental conditions with low O_2 partial pressure, high radiation, extreme intraday thermal oscillations, and freshwater-to-hypersaline conditions (Dorador et al., 2020; Hernández et al., 2016). These systems have salt crusts surrounding the saline lakes, whose water supply comes mainly from groundwater (de la Fuente & Niño, 2010; Marazuela et al., 2019). Even though saline lakes can be found on all continents, high-altitude saline lakes are found mainly on the Tibetan plateau and in the South American highlands (Finlayson, 2018). In South America, saline lakes can be found above 3000 m.a.s.l in the central depressions of endorheic basins in the altiplanic zones of Chile, Bolivia, Peru, and Argentina.

These dynamic ecosystems are characterized by microbial communities that intensely recycle nutrients that limit gross primary production (GPP) (Gao et al., 2021; Huang et al., 2023; Yue et al., 2021). At the trophic base, diatoms and cyanobacteria govern the lake's carbon dioxide and oxygen fluxes (de la Fuente, 2014; Dorador et al., 2020; Paquis et al., 2023). Saline lakes are of great ecological value, as they are oases that are home to a wide variety of species that have physiological and biochemical mechanisms that allow them to tolerate the extreme conditions of arid regions but are very sensitive to even small changes in climate (Finlayson, 2018). However, these aquatic systems are threatened by an increased demand for high-value minerals (e.g., lithium) and extractions from groundwater sources (Halkes et al., 2024; Marazuela et al., 2019). In the case of hypersaline lagoons (>40 g/L), these are considered natural laboratories with unique scientific value because they host a high biodiversity with simple trophic networks compared to other aquatic systems (Gajardo & Redón, 2019).

Saline lakes play a vital role in the context of climate change, as the microbial activity present in these systems contributes to the recycling of greenhouse gases (GHG) through different processes (e.g., carbon fixation, nitrification, and methanogenesis), causing the lakes to act as sinks/sources of these gases (Dorador et al., 2020; Molina et al., 2018; Tranvik et al., 2009). Additionally, climate change could modify the physical conditions of these environments, unbalancing the local water cycle and natural biochemical processes (Uribe Rivera et al., 2017).

Higher temperatures and changes in evaporation and precipitation may cause salinity limits to increase beyond the tolerance of invertebrates, such as brine shrimp (*Artemia spp.)* and brine flies (*Ephedra spp*.) that are part of the food base of birds, especially flamingos. In addition, lake desiccation results in extensive sources of fine dust that can threaten human health (Wurtsbaugh et al., 2017).

On-site monitoring studies are often done to understand how the meteorological forcings affect the dynamics of nutrients, carbon dioxide, and oxygen in complex systems, such as high-altitude saline lakes. The 2018 E-DATA (Evaporation Caused by Dry Air Transport over the Atacama Desert) field campaign was conducted in the Salar del Huasco to investigate the relationship

between meteorological conditions and biochemical dynamics in the open waters of the saline lake (Suárez et al., 2020). Suárez et al. analyzed the effects of wind on the CO_2 flux across the air-water interface. They found there is a strong correlation between wind regimes, evaporation, and biochemical processes present in the Salar del Huasco, emphasizing that climate change may affect wind patterns. De La Fuente (2014) found diurnal meteorological cycles in which wind impacts heat and mass transfer between the Salar del Huasco's lake and the atmosphere. For instance, during the nights and mornings, the water surface is characterized by calm conditions and low sediment resuspension. However, during the afternoon, windy conditions dominate, promoting sediment resuspension and exchanges between the air-water interface (AWI) and water-sediment interface (WSI) (de La Fuente, 2014). The seasonal cycle that characterizes precipitation in the Altiplano is dominated by changes in zonal flow, where easterly winds favor wet conditions (summer) and westerly winds cause dry conditions (winter) (Garreaud et al., 2003). Other studies have indicated that atmospheric circulation is a dominant factor controlling surface fluxes in the desert (e.g., evaporation) and discard radiative energy as the main limiting factor (Aguirre-Correa et al., 2023; Lobos-Roco et al., 2021).

As previously mentioned, microorganisms play a key role in GHG recycling and influence the balance of organic matter and energy in saline lakes. The magnitude, flux, and direction (source or sink) of GHGs in saline lakes have temporal dynamics that are affected by seasonal changes related to temperature, radiation, wind, and available water, which generate variations in microbial communities (Dorador et al., 2020; Molina et al., 2021). There is a complex interaction between environmental factors and water quality and dynamics of saline lakes. For example, in two shallow saline lakes (Lake Los Flamencos, Chile and Lake Khalina, Bolivia), intricate relationships were found between seasonal temperature fluctuations and water quality variables such as salinity, turbidity, and phytoplankton biomass concentration (De los Rios-Escalante et al., 2024). Another study in the Salar del Huasco indicates that the active role of microbial communities can be affected by seasonality (wet and dry periods) that generates alterations in the physical and chemical conditions of the water, causing an unbalance in the ecosystem (Paquis et al., 2023).

While short-term studies have provided valuable insights into saline lakes, particularly on an intraday scale, it is imperative to delve into the long-term behavior of these systems, as environmental factors influencing vertical fluxes, microbial activity, and carbon sequestration/storage may vary at seasonal or annual scales (Molina et al., 2021; Pardo-Esté et al., 2023; Richardson et al., 2024). Computational modeling becomes an essential tool to understand the behavior of these complex systems, considering that monitoring the different processes in extreme places, such as high-altitude saline lakes, and predicting their effects due to climate change are not always feasible. The long-term perspective allows for reaching a state where balances and cycles that characterize the system's response are independent of the initial conditions.

This work aims to study the influence of climatic trends of meteorological variables in high-altitude saline lakes and their relationship with the mechanism governing CO_2 and O_2 concentrations in the water column. Particular interest is given to CO_2 and O_2 transport through

air-water and water-sediment interfaces, consumption/production processes related to primary production, and the effects of meteorological forcing on water quality. We built a 0-dimensional transient model to analyze fluxes and concentrations of CO_2 and O_2 in the water column of the Salar del Huasco in the long term (1948-2021) and to study CO_2 and O_2 dynamics at intraday, daily, monthly, annual, and seasonal scales.

To calibrate the model, we used meteorological and water quality data from two field campaigns (2016 and 2018) and the results from a long-term study in high Andean shallow saline lakes by de la Fuente and Meruane (2017). The present study provides a valuable tool for modelers looking to understand the effects of environmental factors related to climate change on aquatic systems.

2. Materials and methods

2.1. Study site

The Salar del Huasco (hereinafter Salar) is located at 3,800 m above sea level in an endorheic basin north of Chile (20°18'18"S, 68°50'20"W) (Figure 1). This place is recognized as one of the most pristine wetlands of Chile and is a habitat with highly endemic biodiversity (Decreto No. 66, 2023). The fauna includes a variety of camelids and birds, including the Chilean Flamingo (*Phoenicopterus chilensis*), the Andean Flamingo (*Phoenicoparrus andinus*), and the James's Flamingo (*Phoenicoparrus jamesi*) (Caziani et al., 2007; de la Fuente, 2014).

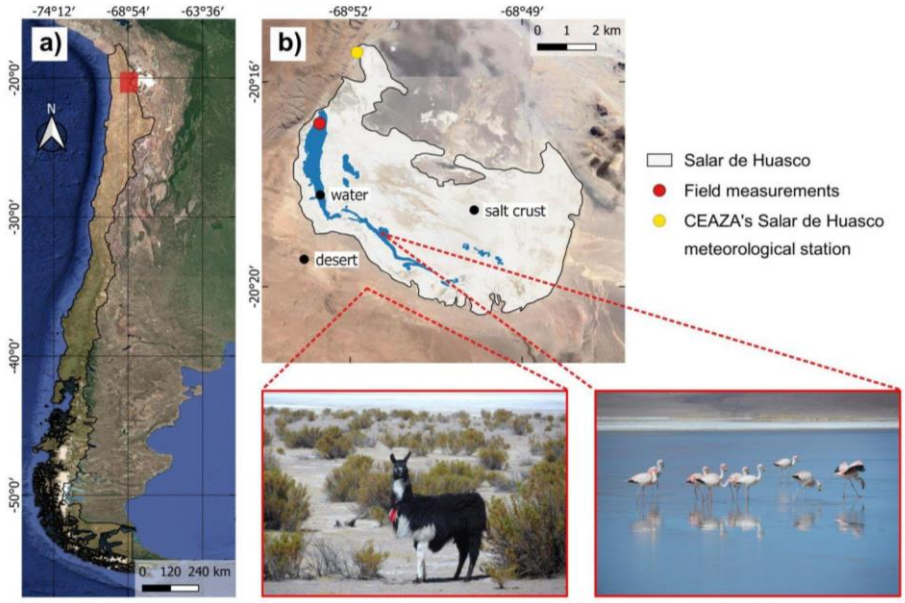

Figure 1. Map of the Salar de Huasco. a) Location of the Salar in Chile. b) Detail of the Salar, sampling site, and CEAZA's Salar del Huasco meteorological station.

In 1996, the Salar was declared as a wetland of international importance and was included in the list of RAMSAR-protected sites. Later, in 2023, it was decreed as a National Park (Decreto No. 66, 2023). The Salar is characterized by temperatures (T_a) ranging from -20°C to 20°C, maximum daily irradiation (R_{sw}) around 1000 $\frac{W}{m^2}$, average relative humidity ($RH\%$) of 42% (Centro de Estudios Avanzados en Zonas Áridas [CEAZA], n. d.), and wind speeds (U_w) up to 16 $\frac{m}{s}$ (Lobos-Roco et al., 2022a). Hourly data for T_a, R_{sw}, $RH\%$, and U_w from 2015 to 2021 is summarized in Figure 2 and the seasonal behavior of these variables is shown in Figure 3. The average annual precipitation is 135 $\frac{mm}{yr}$, and potential evaporation is 1285 $\frac{mm}{yr}$ (de la Fuente et al., 2021).

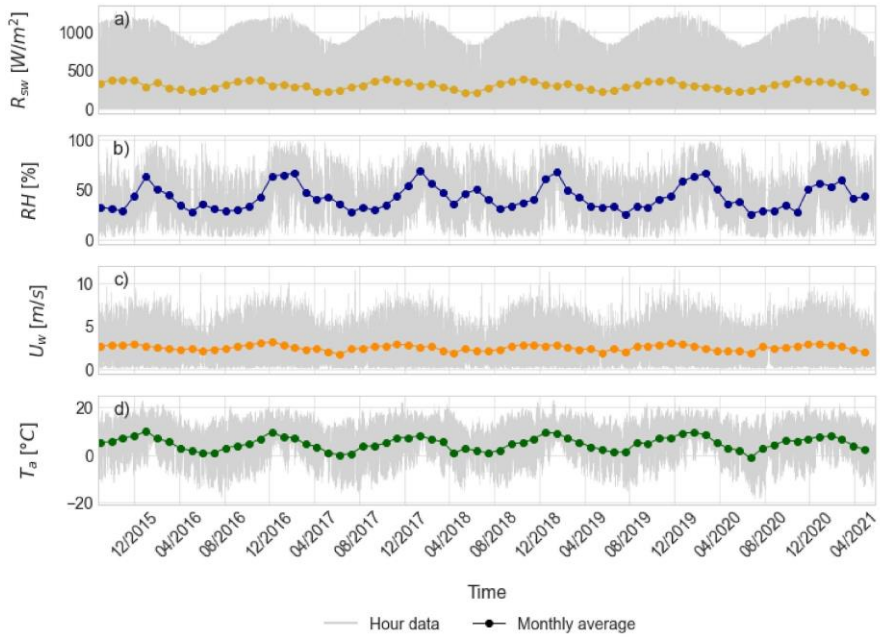

Figure 2. Hourly data (gray solid lines) and monthly averages (coloured lines) of a) solar radiation, b) relative humidity, c) wind speed, and d) air temperature. Data obtained from the public repository CEAZA's Salar del Huasco meteorological station (CEAZA, n. d.).

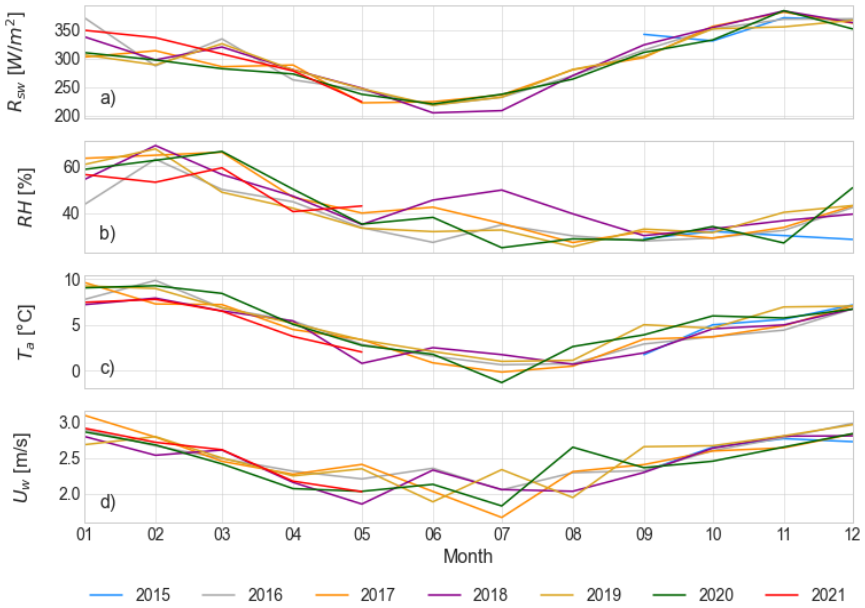

Figure 3. Monthly averages for a) solar radiation, b) relative humidity, c) wind speed, and d) air temperature show the seasonal variation in the study area. Data obtained from the public repository CEAZA's Salar de Huasco meteorological station (CEAZA, n. d.).

2.1.1. Field measurements

Data were collected during field campaigns in the austral autumn 2016 (May) and spring 2018 (November). Located at the water sampling site (Figure 1), a sonic anemometer with a built-in infrared gas sensor (IRGASON, Campbell Sci., Logan, UT, USA) collected the following measurements: $F_{CO2,}$ across the air-water interface, wind speed (U_w), air temperature (T_a), relative humidity ($RH\%$), atmospheric pressure (P), and CO_2 concentration in the air ($[CO_2]_{air}$). Water temperature (T_w), electrical conductivity (EC), and dissolved oxygen concentration ($[O_2]_{aq}$) were measured using a HOBO U26 data logger (Onset Computer Corporation, Bourne, MA, USA). Solar radiation data (R_{sw}) were collected using a CNR4 Net radiometer (Kipp & Zonen, Delft, The Netherlands).

2.2. Model of CO_2 and O_2 dynamics

We used a 0-dimensional impermanent model to simulate the intraday variation of dissolved CO_2 and O_2 in the Salar's water column, as well as the fluxes of CO_2 and O_2 across the air-water interface (AWI) and the water-sediment interface (WSI). The model integrates mass balances for the control variables $[CO_2]_{aq}$, $[O_2]_{aq}$, biomass (B), and detritus (DET) (Equations 1 to 4). The study by Hull et al. (2008) was used to develop this model. Figure 4 shows a schematic of the Salar and the interactions between control variables. Details about the mathematical formulation for each process and fluxes are presented in the Appendix.

According to observations made in the study area, the surface of the saline lake freezes during the night, impeding mass exchanges between the atmosphere and the water column. This condition is considered within this model, and freezing is assumed to occur when the water temperature values are below 0°C.

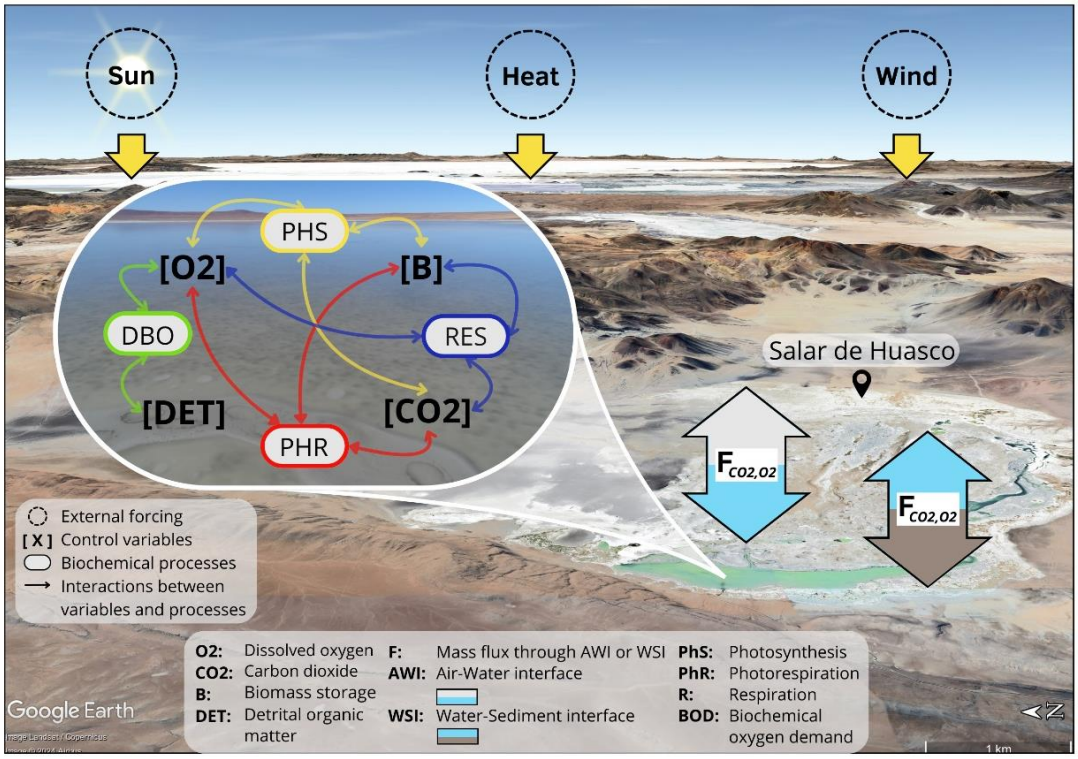

Figure 4. Diagram of processes (transport and biochemical) and control variables present in the model.

2.2.1. Dissolved oxygen concentration

The main processes and fluxes affecting the concentration of O_2 in the water phase are described in Equation 1.

$$\frac{d[O_2]_{aq}}{dt} = nPhS + \frac{F_{O_2,AWI}}{h_w} + \frac{F_{O_2,WSI}}{h_w} - BOD - Res - c \quad (1)$$

where, h_w is the depth of the water phase, $nPhS$ is the net $[O_2]$ contribution due to photosynthetic processes, $F_{O_2,AWI}$ is the flow of $[O_2]$ across the AWI due to reaeration, $F_{O_2,WSI}$ is the oxygen exchange at the WSI, BOD is the biological oxygen demand, and Res is the contribution due to biomass respiration. Specific processes involved in the $[O_2]$ mass balance are:

- Net photosynthesis, $nPhS$: it represents an oxygen production/consumption term resulting from the contribution of photosynthesis minus photorespiration. This process depends on temperature, solar radiation, available carbon dioxide, and nutrient limitation, which is related to the trophic state of the lake and is represented by the dynamics of biomass (B)

expressed in terms of chlorophyll-a.

- Reaeration, $F_{O_2,AWI}$: corresponds to the oxygen exchange between the atmosphere and the water body. This process depends on the concentration of oxygen present in the water column, is governed by physical exchanges, and is influenced by the wind regime.
- Biological oxygen demand, BOD : denotes the microbial degradation of organic matter in water. It depends on the water temperature and the concentration of available organic detritus (DET) that corresponds to the substrate for the process.
- Respiration, Res : corresponds to mitochondrial respiration, a metabolic process carried out by biomass that depends on temperature and organic matter concentration.
- Oxygen exchange at the WSI, $F_{O_2,WSI}$: corresponds to a model of oxygen exchange at the water-sediment interface. This flux is influenced by turbulence in the water column. It also depends on diffusive transport within the sediments and the rate at which biochemical processes produce and consume dissolved oxygen.
- Extra O_2 consumption, c : corresponds to a process associated with O_2 consumption in the water column that is included to simulate the rapid declines observed in $[O_2]_{aq}$ values measured in the field, where anoxic conditions are reached.

2.2.2. Dissolved carbon dioxide concentration

For CO_2 in the water phase, the main processes and fluxes affecting its concentration are shown in equation 2.

$$\frac{d[CO_2]_{aq}}{dt} = \frac{F_{CO_2,WSI}}{h_w} + \frac{F_{CO_2,AWI}}{h_w} + Res - nPhS * k_{O_2-CO_2} \quad (2)$$

where $F_{CO_2,WSI}$ is CO_2 flux at the WSI, $F_{CO_2,AWI}$ is the carbon dioxide exchange at the AWI, *Res* is the contribution due to biomass respiration, $nPhS$ is the net CO_2 contribution due to photosynthetic processes, $k_{O_2-CO_2}$is the constant relating the rates at which CO_2 consumption occurs as a function of O_2 production due to photosynthesis, and h_w is the depth of the water phase. Specific processes involved in the CO_2 mass balance are:

- Carbon dioxide exchange at the AWI, $F_{CO_2,AWI}$: corresponds to the carbon dioxide flux between the aqueous and gas phases. It depends on the concentration of carbon dioxide present in the water column, is governed by physical exchanges, and is influenced by the wind regime.
- Carbon dioxide exchange at the WSI, $F_{CO_2,WSI}$: corresponds to a model of carbon dioxide flux through the sediment-water interface. This flux is influenced by turbulence in the water column. It also depends on diffusive transport within the sediments and the rate at which biochemical processes produce and consume carbon dioxide.

- Net photosynthesis, $nPhS$: it represents an oxygen production/consumption term resulting from the contribution of photosynthesis minus photorespiration. This process depends on temperature, solar radiation, available carbon dioxide, and nutrient limitation, which is related to the trophic state of the lake and is represented by the dynamics of biomass (B) expressed in terms of chlorophyll-a.
- Respiration, Res : corresponds to mitochondrial respiration, a metabolic process carried out by biomass that depends on temperature and organic matter concentration.

2.2.3. Biomass concentration

The main processes and fluxes affecting the concentration of B in the water phase are described in Equation 3.

$$\frac{d[B]}{dt} = Grow_{wat} + Grow_{sed} - Loss_{wat} - Loss_{sed} \quad (3)$$

where $Grow_{wat}$ and $Loss_{wat}$ are growth and loss of biomass in the water column and $Grow_{sed}$ and $Loss_{sed}$ are growth and loss in the sediments. The specific processes involved in the biomass balance are described below:

- Growth of biomass in water, $Grow_{wat}$: biomass growth is related to primary production in the water column; therefore, it depends on net photosynthesis.
- Growth of biomass in sediments, $Grow_{sed}$: corresponds to the growth of biomass associated with primary producers in the sediments. This depends on the net oxygen production in the sediments.
- Loss of biomass in water, $Loss_{wat}$: corresponds to the loss of biomass in the water column. Biomass loss is due to natural death and is obtained by considering the decay rate of the living biomass. The biomass concentration in the water will depend on the percentage of sediment resuspension.
- Loss of biomass in sediments, $Loss_{sed}$: corresponds to the loss of biomass in the sediments. In this case, the biomass concentration will depend on the percentage of sediment that is not resuspended by the wind.

2.2.4. Detritus concentration

The processes associated with detrital concentration in the water column are shown in Equation 4.

$$\frac{d[DET]}{dt} = Loss_{wat} + Loss_{sed} - BOD - \bar{r} \quad (4)$$

where $Loss_{wat}$ and $Loss_{sed}$ are the loss of biomass in the water and sediments, BOD is the

biological oxygen demand, and $\bar{r}$ is the rate of oxygen consumption in the sediments. Dead biomass increases the amount of substrate, while the degradation of organic matter consumes that substrate. The specific processes involved in the detritus balance are described below:

- Loss of biomass in water, $Loss_{wat}$: corresponds to the loss of biomass in the water column. Biomass loss is due to natural death and is obtained by considering the decay rate of the living biomass. The biomass concentration in the water will depend on the percentage of sediment resuspension.
- Loss of biomass in sediments, $Loss_{sed}$: corresponds to the loss of biomass in the sediments. In this case, the biomass concentration will depend on the percentage of sediment that is not resuspended by the wind.
- Biological oxygen demand, BOD : denotes the microbial degradation of organic matter in water. It depends on the water temperature and the concentration of available organic detritus (DET) that corresponds to the substrate for the process to take place.
- Oxygen consumption in sediments, $\bar{r}$: corresponds to the rate of consumption within the active layer δ_p. This consumption includes respiration by photosynthetic microorganisms, respiration by bacteria, and oxygen uptake due to inorganic chemical reactions.

To solve the differential equations mentioned above, we use the Runge-Kutta numerical method, which corresponds to a high-precision iterative method that allows to determine the solution at time $t = t_{i+1}$ from the solution at time $t = t_i$. Details on this method and the equations used can be found in "Numerical Methods for Engineers" by Chapra and Canale (2015).

2.3. Model data

To simulate historical trends of O_2 and CO_2 concentrations in the water column, we used input data from de la Fuente and Meruane (2017) from 1950 to 2020. De la Fuente and Meruane used a spectral model to simulate long-term thermodynamics in shallow wetlands, specifically in the Salar del Huasco. The data include water temperature (T_w), solar radiation (R_{sw}), atmospheric pressure (P), air temperature (T_a), wind shear velocity (u_c), and specific humidity (q). For verification, Figure 5 compares the simulated data by de la Fuente and Meruane (2017) with the data measured in the field. While Figures 5 a), c), and e) show de la Fuente and Meruane's long-term simulated series of T_a, T_w, and U_w, Figures 5 b), d), and f) show a close-up comparison with the field campaign conducted in November 2018.

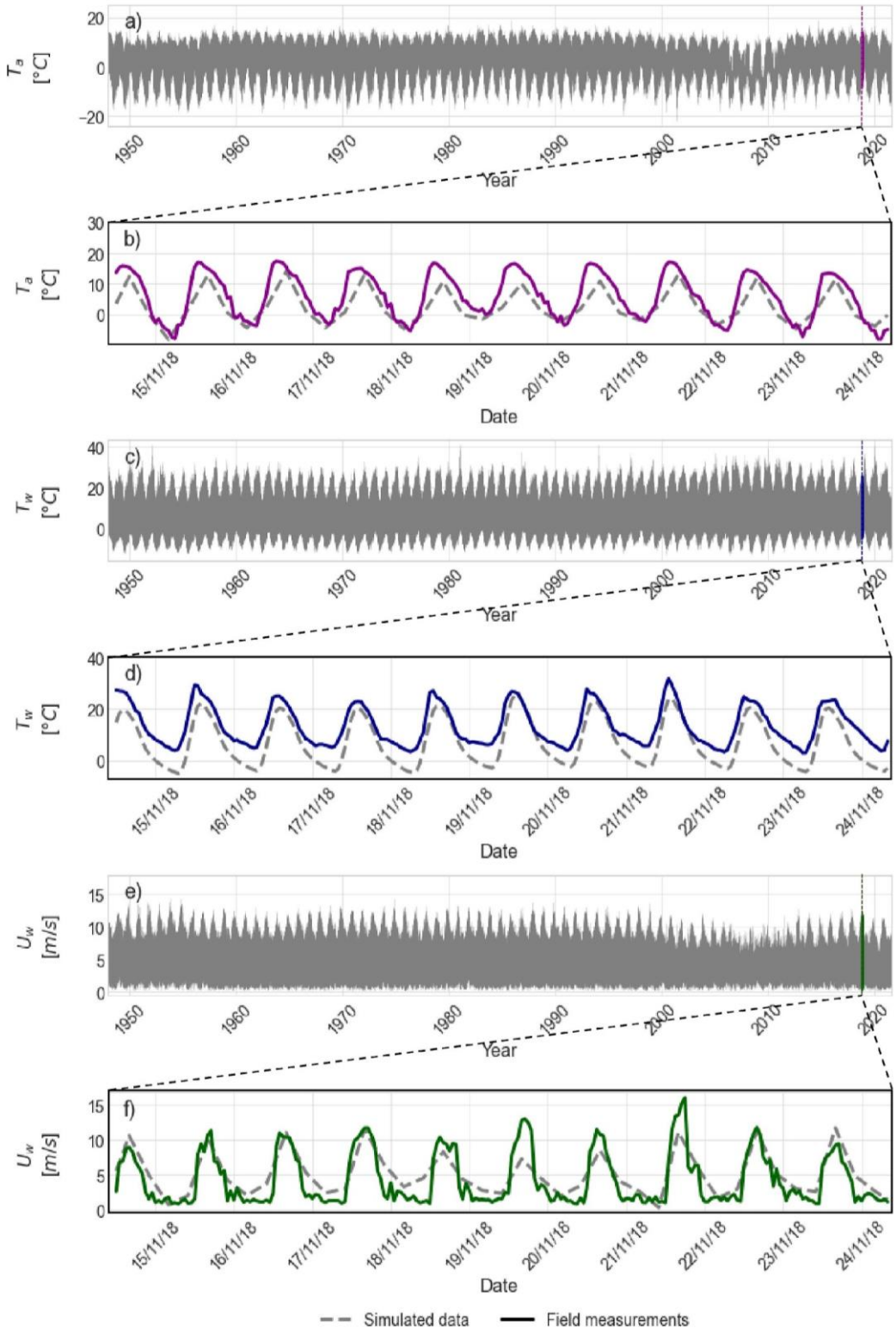

Figure 5. Verification between the simulated data by de la Fuente and Meruane (2017) and field measurements. Panels a), c) and e) show the simulated long-term series for of T_a, T_w, and U_w, respectively. Panels b), d), and f) show the simulated (gray line) and measured (colored lines) data for November 2018.

2.4. Sensitivity analysis and calibration of parameters

The parameters present in the model are calibrated using values obtained from the literature. This calibration was performed using dissolved O_2 and $F_{CO_2,AWI}$ measured data in two field campaigns conducted in the Salar in 2016 and 2018. It is important to consider that there are no measured concentration data in the water column for all the control variables and no measurements in the different seasons of the year, which may influence the calibration and precision of the results.

The calibrated parameters were used to perform a global sensitivity analysis to determine the most relevant processes associated with $[O_2]_{aq}$ and $[CO_2]_{aq}$. We used Sobol's index, an analysis based on dividing the result's variance into fractions corresponding to individual contributions of input variables to the total variance (Sobol, 2001). Sobol's indices can be estimated depending on whether interactions between variables are considered.

First-order indices correspond to the direct contribution of each input variable to the output variable. Higher-order indices include the joint effect of two or more input variables on the output. The sum of all the indices associated with an output variable equals 1. In this case, we used the first-order indices to find the individual influence of each process on the control variables.

Figure 6 presents the first-order indices associated with each source/consumption term for oxygen and carbon dioxide in the water column. We used the Python Sensitivity Analysis Library (SALib) for these calculations. Since we have a time series for control variables and processes, the sensitivity analysis generates a sensitivity time series. The mean values of these series are shown in Figure 6. Lighter colors indicate less influence of the process on the control variables, and darker colors indicate a more significant effect.

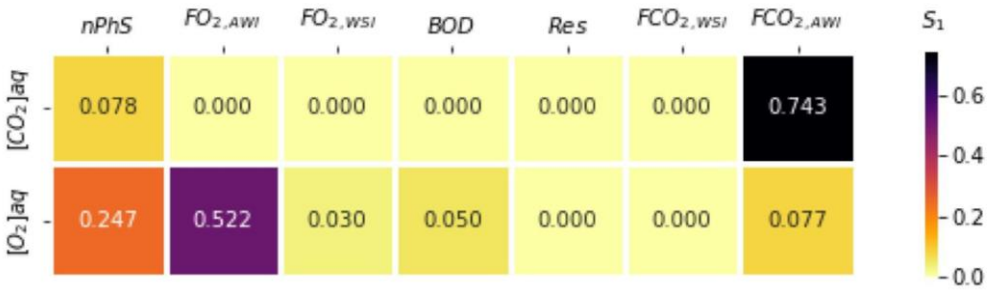

Figure 6. First-order Sobol index values (S_1) associated with each process related to the control variables $[O_2]_{aq}$ and $[CO_2]_{aq}$.

The sensitivity analysis results indicate that the processes that have the most significant influence on $[CO_2]_{aq}$ are mass exchange between air-water interfaces $(F_{CO_2,AWI})$ and net photosynthesis $(nPhS)$. In the case of $[O_2]_{aq}$, it is observed that the main processes are the flux through the AWI $(F_{O_2,AWI})$ and net photosynthesis. Figure 6 shows that the sum of the indices for

$[CO_2]_{aq}$ is 0.821, and for $[O_2]_{aq}$ is 0.926 (both values less than 1), which implies that there are interactions between parameters (higher order indices) that influence the output variables.

A second calibration is carried out, focusing on the parameters associated with the most significant processes. A 70-year modeling is performed for different parameter combinations to obtain the best fit between simulated and measured data. A total of 3,000 samples were obtained, and each sample's root mean square error (RMSE) was calculated. The 100 samples with the lowest RMSE were used to obtain the final values of the calibrated parameters. The parameters associated with these samples were averaged and are presented in Table 1. The range of RMSE values for the 100 samples was 0.0022 to 0.0027 $\left[\frac{mg \cdot m}{L \cdot min}\right]$ for $F_{CO_2,AWI}$ and 3.02 to 4,09 $\left[\frac{mg}{L}\right]$ for $[O_2]_{aq}$.

Table 1: Calibrated parameter values used in the final model (mean $\pm$ standard deviation)

	Parameter	**Value range**	**Reference**	**Calibrated value**	**Unit**
	C/chlorophyll-a ratio for algae	0.05	(Jørgensen et al., 1991)	0.03 ± 0.003	$\frac{mg\ C}{mg\ Chla}$
μ_{max}	O_2 max production rate	0.0585 - 1.944	(Hammer, 1981)	1.73 ± 0.22	$\frac{mg\ O_2}{mg\ Chla\ \cdot\ min}$
α_{PhR}	O_2 max consumption rate	0.0583	(Hull et al., 2008)	0.06 ± 0.01	$\frac{mg\ O_2}{mg\ Chla\ \cdot\ min}$
θ_{PhS}	Temperature correction factor (photosynthesis)	1.036	(Hull et al., 2008)	1.11 ± 0.06	-
θ_{PhR}	Temperature correction factor (photorespiration)	1.08 - 1.47	(Hull et al., 2008), (Stefan & Fang, 1994)	1.09 ± 0.13	-
α_{Rsw}	Half-saturation constant for radiation in photosynthesis	50	(Hull et al., 2008)	54.4 ± 5.6	$\frac{W}{m^2}$
β_{Rsw}	Half-saturation constant for radiation in photorespiration	150	(Hull et al., 2008)	150.8 ± 20.3	$\frac{W}{m^2}$
k_{O_2}	Half-saturation constant for oxygen	2.5	(Hull et al., 2008)	2.56 ± 0.33	$\frac{mg\ O_2}{l}$
k_{CO_2}	Half-saturation constant for carbon dioxide	3.4 - 5	(Burkhardt et al., 2001)	3.57 ± 0.44	μM
A_{O_2}	Constant to calculate the O_2 transfer rate through AWI	-	Calibrated	0.30 ± 0.04	-
A_{CO_2}	Constant to calculate the CO_2 transfer rate through AWI	-	Calibrated	1.03 ± 0.11	-

3. Results

3.1. Model prediction

Long-term simulated physical and biochemical processes related to O_2 and CO_2 dynamics in the Salar's water column are presented in Figures 7 and 8, respectively. Figures 7 and 8 also show a comparison between measured data and the simulated variables. Figure 7b shows the hourly values (gray line) and the annual averages (blue line) of dissolved O_2 simulated for 70 years; both curves were obtained from the average of the 100 best samples. The annual average concentration remained close to 3 $\frac{mg}{L}$ throughout the entire series and hourly level there was a variation in the trend between the years 2005 and 2015.

A close-up comparison between the simulations (blue lines) and the measured data (green lines) is shown in Figures 7a and 7c. The blue shaded area in all panels corresponds to the 95% confidence interval associated with the 100 samples with the lowest RMSE. The simulation indicates lower O_2 concentrations during the early morning, where anoxic states are reached, and concentrations close to 5 $\frac{mg}{L}$ at midday for both field campaigns. For the 2016 data set (Figure 7a), the simulation underestimates the maximum values of dissolved O_2 concentrations. While for the 2018 campaign, a simulated series closer to the field measurements is observed (Figure 7c).

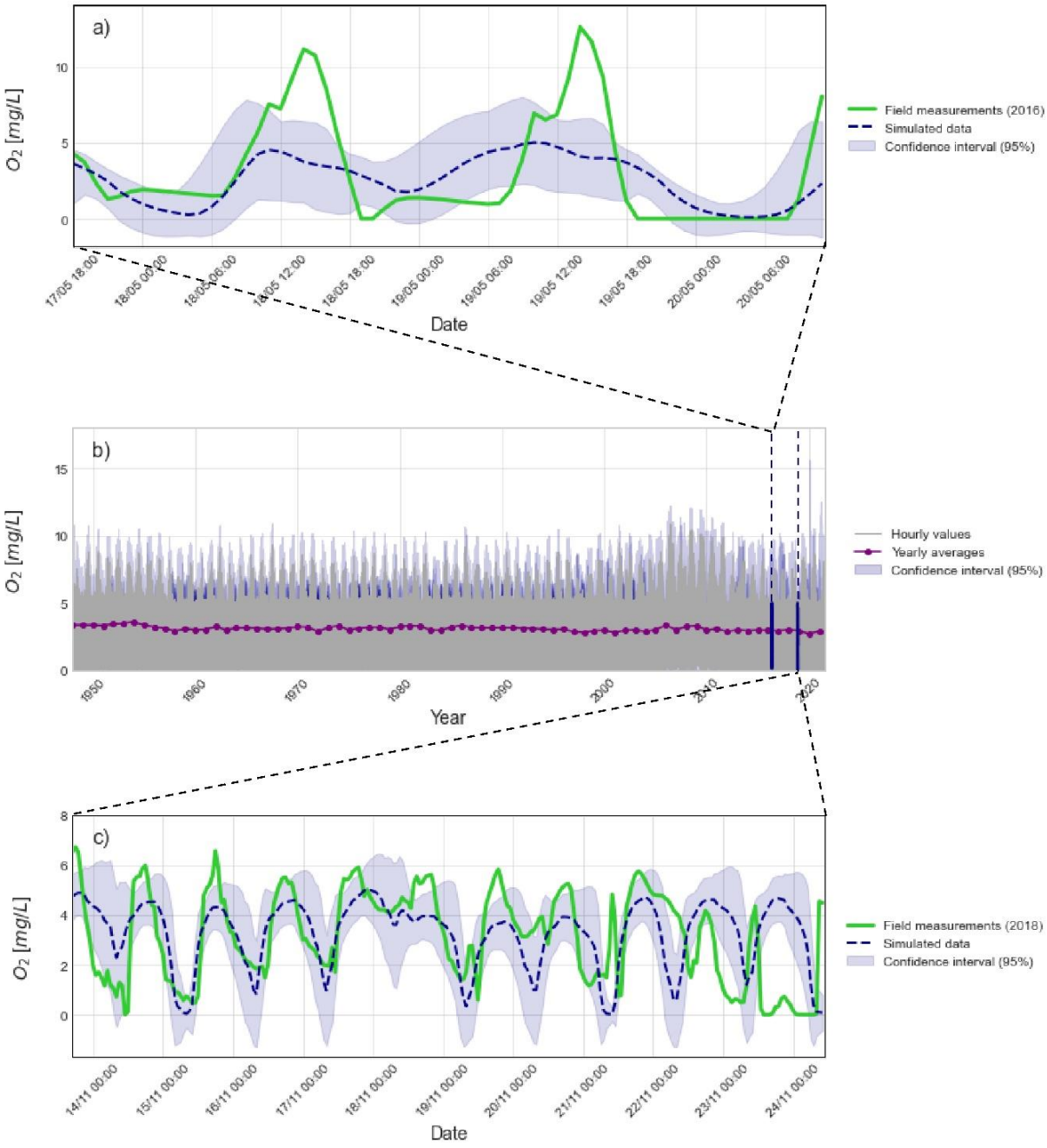

Figure 7. Long-term simulation results for $[O_2]_{aq}$. (b) Hourly values (gray line) and annual averages (blue line). Comparison between simulated values and field campaigns data from May 2016 (a) and November 2018 (c).

Figure 8b shows the hourly values (gray line) and the annual averages (red line) of CO_2 fluxes at the AWI simulated for 70 years, both curves were obtained from the average of the 100 best samples. The annual average concentration remained close to 0.001 $\frac{mg \cdot m}{L \cdot min}$ throughout the entire series.

A close-up comparison between the simulations (brown lines) and the measured data (yellow lines) is shown in Figures 8a and 8c. The brown shaded area in all panels corresponds to the 95% confidence interval associated with the 100 samples with the lowest RMSE. The simulation indicates a CO_2 flux close to zero at the AWI during the morning and a positive flux (entering the lake) during the afternoon, reaching values of 0.003 $\frac{mg \cdot m}{L \cdot min}$ for the 2016 campaign and 0.005 $\frac{mg \cdot m}{L \cdot min}$ for 2018.

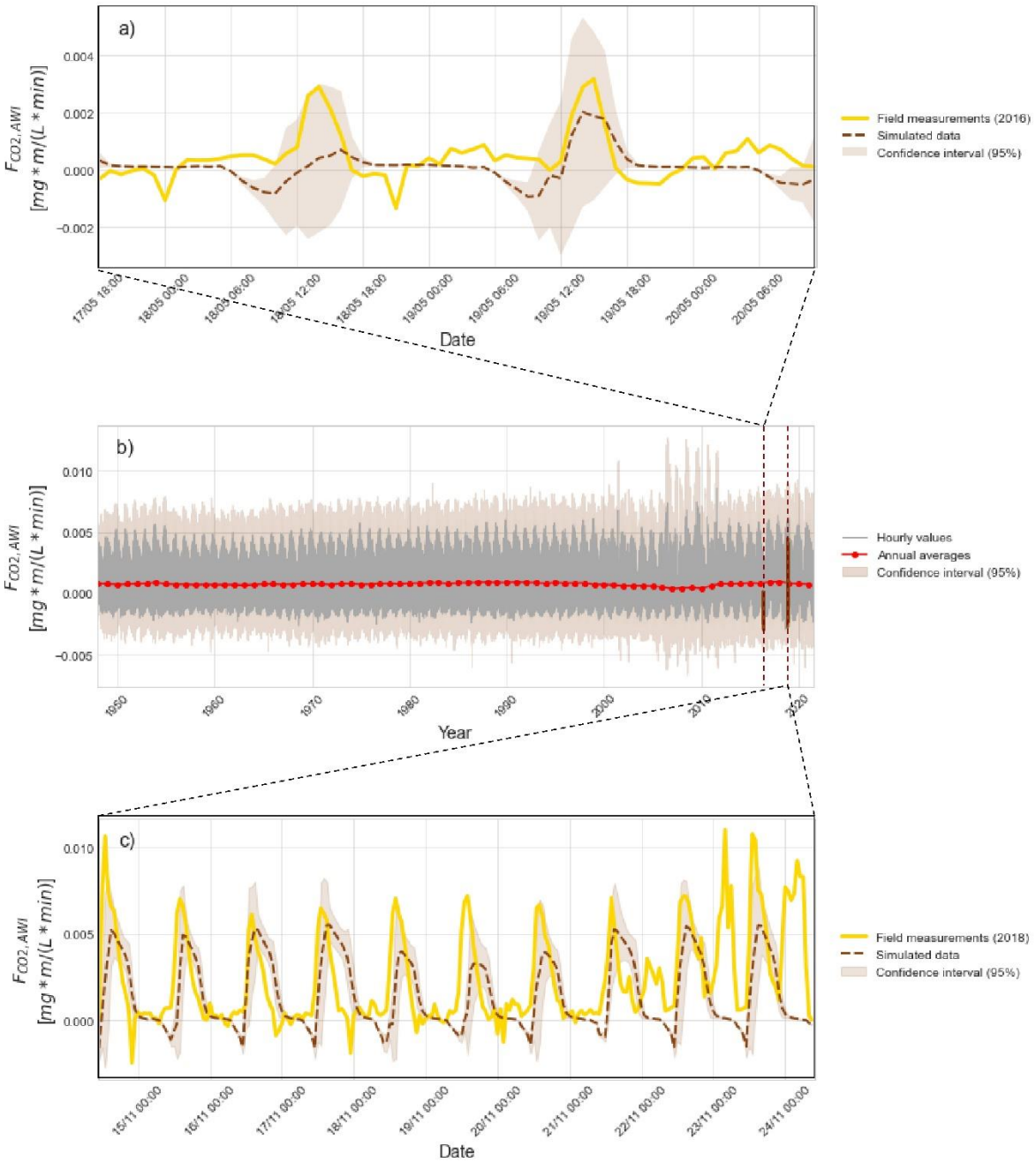

Figure 8. Long-term simulation results for carbon dioxide flux at AWI. (b) Hourly values (gray line) and annual averages (red line). Comparison between simulated values and field campaigns data from May 2016 (a) and November 2018 (c).

3.2. Seasonal variation

The seasonal-scale dynamics of dissolved O_2 and CO_2 concentrations in the water column and CO_2 flux across the AWI are shown in Figure 9. Figure 9a shows that O_2 concentrations do not show significant variations throughout the year, with monthly averages ranging from 2.6 to 3.2 $\frac{mg}{L}$. Regarding CO_2, Figure 9b shows a high seasonal variation, with averages close to 0.6 $\frac{mg}{L}$ in the summer (December to March) and values reaching 1.1 $\frac{mg}{L}$ in June and July.

During winter, low temperatures favor freezing in AWI, limiting effective radiation, resuspension of the active sediment layer, and gas transport processes such as CO_2 flux (Figure 9c).

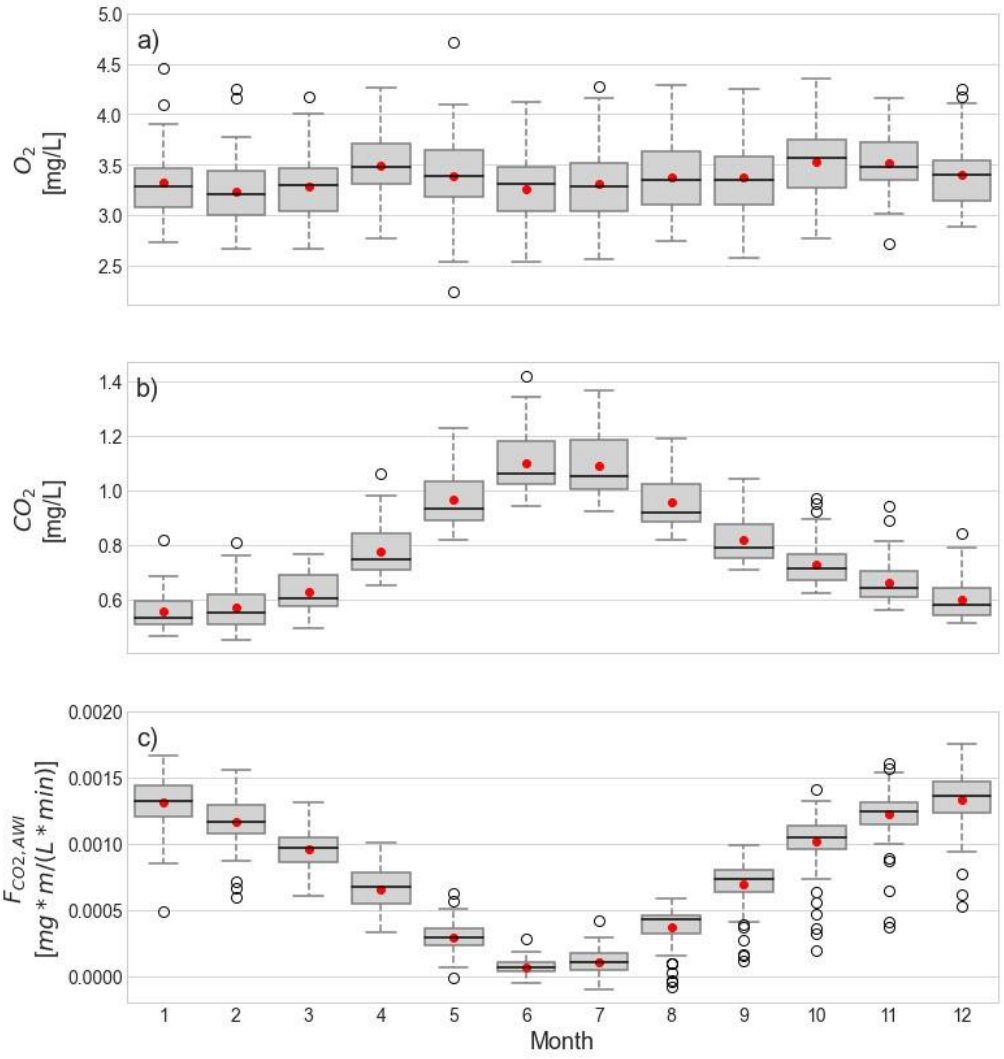

Figure 9. Seasonal variation for O_2 concentration in the water column (a), CO_2 concentration in the water column (b), and CO_2 flux through AWI (c). The boxes represent the quartiles (25% and 75%), the filled red circles are the averages, the horizontal black lines are the medians, the bars represent the maximum and minimum values, and the circles correspond to the outliers.

3.3. Effects of inputs on control variables

One of the main objectives of this work was to study the relationship between meteorological forcings related to climate change and the effects on the quality of aquatic systems, particularly in shallow, high-altitude lagoons. Figure 10 presents a comparison between the principal control variables (CO_2 and O_2), the CO_2 flux through AWI ($F_{CO2,AWI}$), and two variables that were used as inputs to the model (T_a and u_c). The circled lines correspond to the annual average series, and the shaded areas represent the interval between the annual average calculated with the daily maximums and minimums.

Figure 10a shows that the curve of annual averages of $[CO_2]_{aq}$ since 1948 has increased slightly (orange circles). It is observed that the annual minimum curve shows an increase between the years 2005 and 2010. In the case of $[O_2]_{aq}$ (Figure 10b), the curve of annual averages (blue circles) presents values ranging between 2.8 and 3.8 $\frac{mg}{L}$. The annual maximum curve shows an increase in concentration between 2005 and 2010, reaching values above 5 $\frac{mg}{L}$. Figure 10c shows the absolute values of carbon dioxide flux (without direction) through AWI; here, the average curve is constant over time until 2007, when the flux decreases.

Figure 10d shows that the lowest air temperatures occur between 2005 and 2012. In the case of wind speed (Figure 10e), in the year 2000, the curve of average daily maximums begins to decrease, reaching the lowest values in 2007, and the curve of average daily minimums shows an increase in these same years. The figures show that the periods of greater variation of the curves for the output variables coincide with the periods of greater change in the inputs.

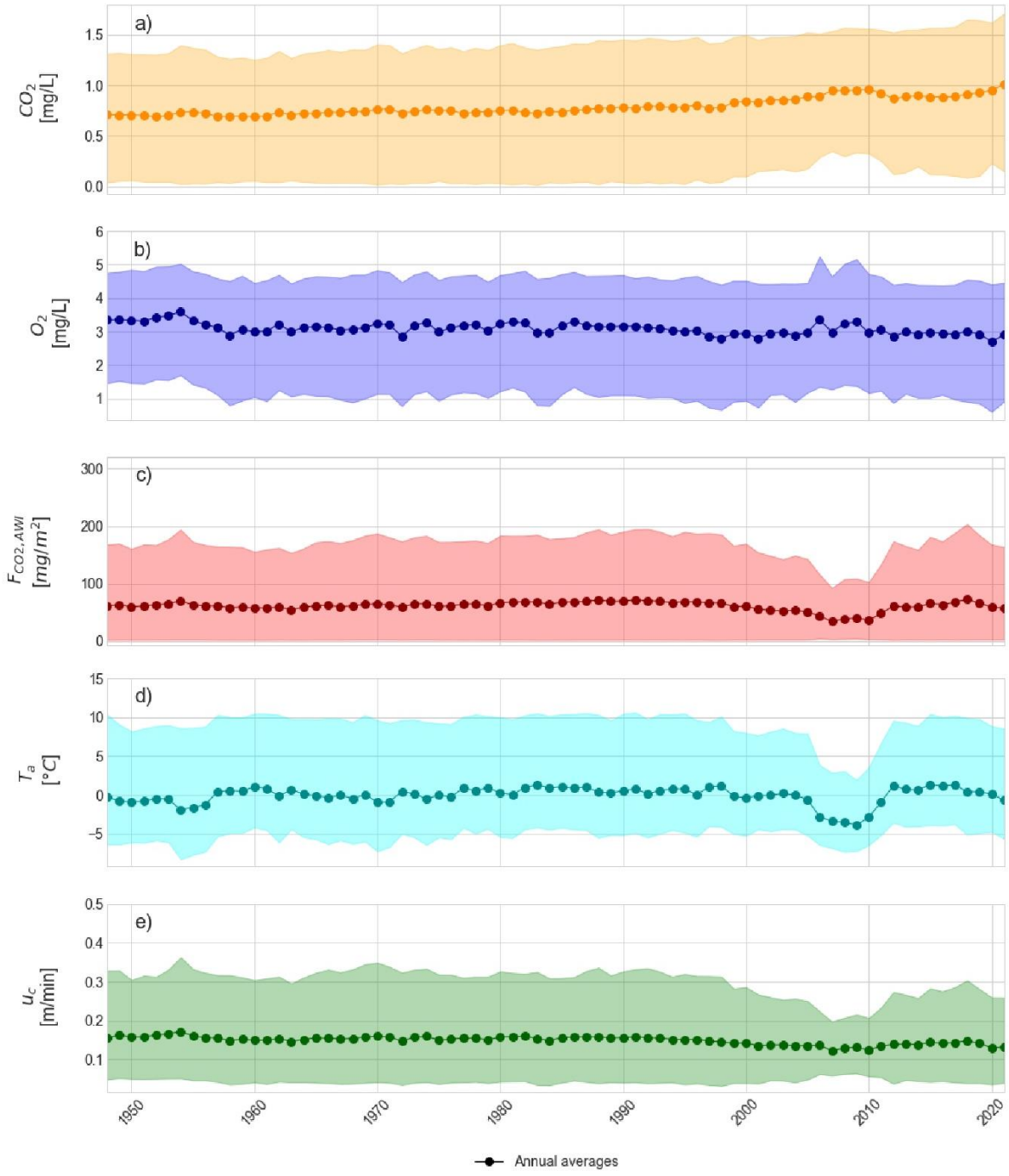

Figure 10. Series of annual averages (circles) and range between annual averages of maximums and minimums (shaded area) for the model outputs: carbon dioxide concentration (a), oxygen concentration (b) and carbon dioxide flux (c); and for the input variables: air temperature (d) and wind shear velocity (e).

Figure 11 shows the effects of the inputs water temperature (T_w) and wind shear velocity (u_c) on the output variables $[CO_2]_{aq}$ and $[O_2]_{aq}$, both of which correspond to variables simulated in the long-term by the spectral model of de la Fuente and Meruane (2017). The hourly series in light gray and the annual averages curve (filled circles) show the behavior of the control variables if a mean water temperature is used as input. The same procedure was carried out with wind shear velocity (dark gray time series and curve with unfilled circles). It was observed that the latter input had a significant influence on the control variables since a greater variation is seen on an hourly scale compared to the series associated with T_w.

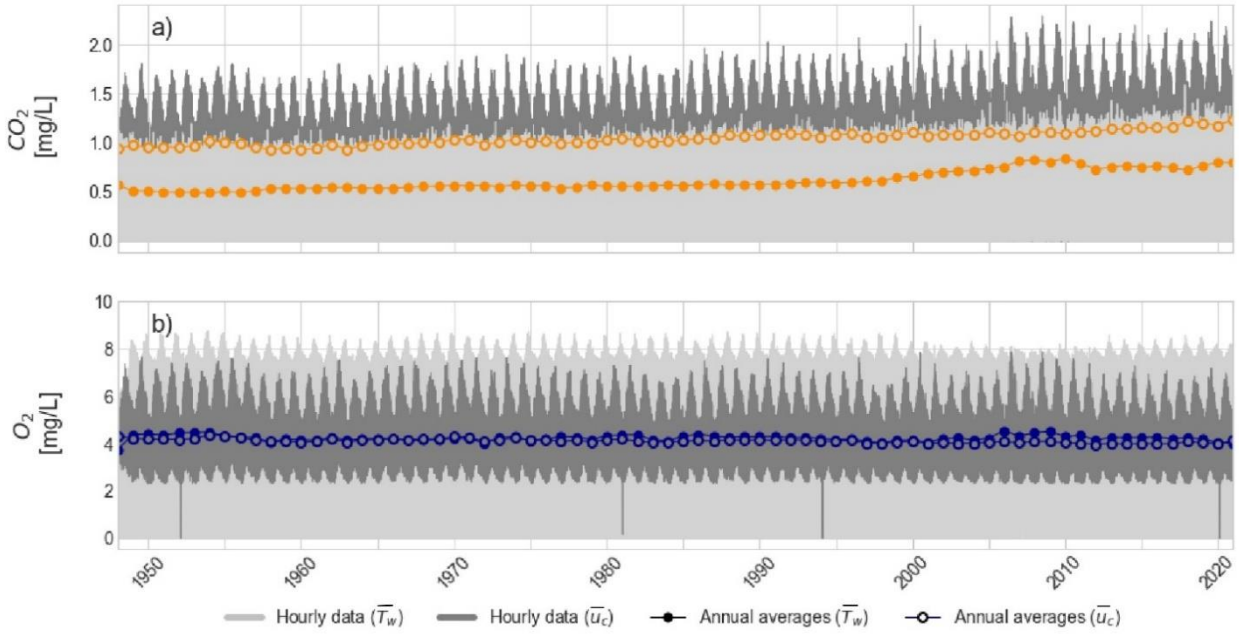

Figure 11. Concentration results for CO_2 (a) and O_2 (b). Gray areas correspond to hourly data calculated with the average shear rate $\overline{u_c}$ (dark gray) and with the average water temperature $\overline{T_w}$ (light gray). The series of circles correspond to the annual averages calculated with $\overline{u_c}$ (unfilled circles) and with $\overline{T_w}$ (filled circles).

4. Analysis and discussion

From the results of the sensitivity analysis, it can be concluded that oxygen and carbon dioxide concentrations depend mainly on physical processes of mass transport between the lake and the atmosphere ($F_{CO_2,AWI}$ and $F_{O_2,AWI}$), and not on biochemical processes. Identifying the main processes allows us to filter the parameters that most influence $[CO_2]_{aq}$ and $[O_2]_{aq}$ variations. It is important to take into consideration that when performing the second calibration with these parameters, the 100 best samples are obtained, which implies that the results are not conditioned to a single sample, as shown in the confidence intervals presented in Figures 7 and 8. Adding to this, these figures show that the model can simulate the intraday dynamics of $[O_2]_{aq}$ and CO_2 flux

through AWI, respectively. The behavior of the $F_{CO_2,AWI}$ during the mornings may be due to the low temperatures that generate freezing on the lake surface, impeding fluxes between the lake and the atmosphere. It is important to take into consideration that, as mentioned above, the inputs used (hourly data) come from the study by de la Fuente and Meruane (2017) where the spectral model presented uses NCEP-NCAR atmospheric reanalysis data, which provides information every 6 hours. De la Fuente and Meruane (2017) indicate that the reanalysis data were linearly interpolated every hour, therefore, variations obtained between the field campaigns and the simulations may be due to the limitations that the spectral model may have on the intraday scale.

One key takeaway from our study is that the model can generate long-term simulations that match field measurements. This capability, coupled with the model's independence from initial conditions, underscores its potential to accurately depict the system's equilibrium associated with mass balances.

Our model also provides key information on the seasonality of the control variables. The results revealed distinct behaviors of CO_2 and O_2 concentrations. For instance, the increased $[CO_2]_{aq}$ during winter is attributed to decreased solar radiation (R_{sw}), which influences photosynthetic processes and subsequent CO_2 consumption by primary producers.

As shown in Figure 10, the model inputs associated with meteorological variables influence the control variables. More importantly, wind speed is a key forcing affecting high-altitude saline lakes on different time scales, especially hourly (Figure 11). Wind not only influences the fluxes analyzed in this model, but previous studies have also found that this variable influences the energy balance of the Salar. During the morning, the latent heat flux is limited by the absence of mechanical turbulence; on the contrary, the arrival of regional wind flow during the afternoon generates an increase in mechanical turbulence triggering high evaporation rates, which rules out radiative energy as the main limiting factor of surface fluxes (Aguirre-Correa et al., 2023; Lobos-Roco et al., 2021; Lobos-Roco et al., 2022b). It is important to note that when we talk about climate change, its effects are mainly related to the increase in ambient temperature. However, wind patterns are also affected, thus affecting the flow and quality of water in aquatic systems.

This study analyzed different processes that may play a role in each control variable's mass balances. However, in the case of $[CO_2]_{aq}$, the model results indicate that the only process that generates variations in concentration within the water column is the flux through the AWI. In addition, most of the positive flux values in Figure 8b suggest that the Salar del Huasco behaves as a sink for atmospheric CO_2, which is also observed in the increase of CO_2 concentration over time (Figure 10a).

5. Conclusions

Salars are habitats with a unique reservoir of biodiversity and play a key role in greenhouse gas cycles. These systems have closed dynamics, which means that any change, however small it may seem, generates effects that greatly influence each other and unbalance the physical, chemical, and biological cycles.

The saline lakes present atmosphere-surface interactions that vary on different time scales and trigger changes in biochemical cycles. In this work, we studied the effects of meteorological forcing on water quality and the processes in these aquatic systems. A transient 0-D model capable of simulating O_2 and CO_2 concentrations in a shallow lagoon of the Salar del Huasco was developed to study the influence of environmental factors on the dynamics of biochemical and transport processes and, thus, on the system's water quality. The results indicate that meteorological factors have significant effects on high Andean wetlands; in particular, it was concluded that one of the main forcings is the wind regime and that a change in this variable can generate greater impacts than fluctuations in temperature. Therefore, it is relevant to consider this variable in climate change studies, especially when performing intraday scale analyses.

It would be interesting to incorporate other processes related to the variables studied in future model versions, such as reactions associated with the carbonate system and anaerobic processes. In addition, as mentioned above, salars play an essential role in climate change; for this reason, other control variables associated with greenhouse gases (e.g., methane and nitrous oxide) could be incorporated, and the behavior of this aquatic system could be analyzed. In addition, it is recommended that more detailed field campaigns be carried out in different seasons of the year to have continuous measurements of all the control variables. Particularly in this study, having CO_2 concentration data would allow for better calibration and thus achieve a more accurate simulation of the processes in Salar del Huasco.

The model presented in this study corresponds to a first approximation of the functioning of this type of aquatic system. It is important to point out that the methodology presented is transferable to simulate processes in lagoons in other parts of the world with the necessary meteorological and water quality information.

6. Author contributions

Karina Valenzuela: Conceptualization, methodology, software, investigation, formal analysis, writing - original draft. **Alberto de la Fuente:** Conceptualization, methodology, software, writing - review & editing, funding acquisition. **Ana Prieto:** Conceptualization, methodology, supervision, writing - review & editing, funding acquisition**. Francisco Suárez:** Data curation, writing - review & editing.

7. Acknowledgements

This research was funded by ANID/FONDECYT/1221191. F. Suárez and A. de la Fuente also acknowledge funding by ANID/FONDECYT/1210221 and ANID/ATE/230006.

8. References

1 Aguirre-Correa, F., de Arellano, J. V. G., Ronda, R., Lobos-Roco, F., Suárez, F., & Hartogensis, O. (2023). Midday Boundary-Layer Collapse in the Altiplano Desert: The Combined Effect of Advection and Subsidence. *Boundary-Layer Meteorology*, *187*(3), 643-671. https://doi.org/10.1007/s10546-023-00790-5

2 Burkhardt, S., Amoroso, G., Riebesell, U., & Sültemeyer, D. (2001). CO_2 and HCO_3^- uptake in marine diatoms acclimated to different CO_2 concentrations. *Limnology and Oceanography*, *46*(6), 1378–1391. https://doi.org/10.4319/lo.2001.46.6.1378

3 Caziani, S. M., Rocha Olivio, O., Rodríguez Ramírez, E., Romano, M., Derlindati, E. J., Tálamo, A., Ricalde, D., Quiroga, C., Pablo Contreras, J., Valqui, M., & Sosa, H. (2007). Seasonal distribution, abundance, and nesting of Puna, Andean, and Chilean Flamingos. *The Condor*, *109*(2), 276–287. https://doi.org/10.1093/condor/109.2.276

4 CEAZA (n. d.). Red de estaciones meteorológicas: CEAZA-Met, Chile. https://www.ceazamet.cl/index.php?pag=mod_mapa&p_cod=ceazamet

5 Chapra, S. C., & Canale, R. P. (2015). *Numerical methods for engineers*. McGraw-Hill Education.

6 Cole, J. J., & Prairie, Y. T. (2009). Dissolved CO_2. In G. E. Likens (Ed.), *Encyclopedia of Inland Waters* (pp. 30–34). Academic Press. https://doi.org/https://doi.org/10.1016/B978-012370626-3.00091-0

7 Decreto No. 66, Crea Parque Nacional Salar del Huasco, en la Región de Tarapacá, y deja sin efecto los decretos N° 24 de 2019 y N° 5 de 2022, no tramitados, Marzo 1, 2023, Diario Oficial [D.O.] (Chile). https://www.diariooficial.interior.gob.cl/publicaciones/2023/03/01/43490/01/2279009.pdf

8 de la Fuente, A. (2014). Heat and dissolved oxygen exchanges between the sediment and water column in a shallow salty lagoon. *Journal of Geophysical Research: Biogeosciences*, *119*(4), 596–613. https://doi.org/10.1002/2013JG002413

9 de la Fuente, A., & Meruane, C. (2017). Spectral model for long-term computation of thermodynamics and potential evaporation in shallow wetlands. *Water Resources Research*, *53*(9), 7696–7715. https://doi.org/10.1002/2017WR020515

10 de la Fuente, A., Meruane, C., & Suárez, F. (2021). Long-term spatiotemporal variability in high Andean wetlands in northern Chile. *Science of the Total Environment*, *756*.

https://doi.org/10.1016/j.scitotenv.2020.143830

11 de la Fuente, A., & Niño, Y. (2010). Temporal and spatial features of the thermohydrodynamics of shallow salty lagoons in northern Chile. *Limnology and Oceanography*, *55*(1), 279–288. https://doi.org/10.4319/lo.2010.55.1.0279

12 De los Rios-Escalante, P. R., Esse, C., Correa-Araneda, F., Rodríguez, L., Fernandez, C.E., Prado, P.E. (2024). Potential Effects of Climate Change in Saline Shallow Lakes in the North of Chile (Salar de Atacama, 23°S, Chile) and South Lipez of Bolivia (Khalina Lake, 22.61°S). In: Singh, A.L., Jamal, S., Ahmad, W.S. (eds) *Climate Change, Vulnerabilities and Adaptation: Understanding and Addressing Threats with Insights for Policy and Practice* (pp. 171–182). Springer Nature Switzerland. https://doi.org/10.1007/978-3-031-49642-4_9

13 Dorador, C., Molina, V., Hengst, M., Eissler, Y., Cornejo, M., Fernández, C., & Pérez, V. (2020). Microbial Communities Composition, Activity, and Dynamics at Salar de Huasco: A Polyextreme Environment in the Chilean Altiplano. In M. E. Farías (Ed.), *Microbial Ecosystems in Central Andes Extreme Environments: Biofilms, Microbial Mats, Microbialites and Endoevaporites* (pp. 123–139). Springer International Publishing. https://doi.org/10.1007/978-3-030-36192-1_9

14 Downing, J. A., Prairie, Y. T., Cole, J. J., Duarte, C. M., Tranvik, L. J., Striegl, R. G., McDowell, W. H., Kortelainen, P., Caraco, N. F., Melack, J. M., & Middelburg, J. J. (2006). The global abundance and size distribution of lakes, ponds, and impoundments. *Limnology and Oceanography*, *51*(5), 2388–2397. https://doi.org/10.4319/lo.2006.51.5.2388

15 Finlayson, C.M. (2018). Salt Lakes. In: Finlayson, C., Milton, G., Prentice, R., Davidson, N. (eds). The Wetland Book: II: Distribution, Description, and Conservation. (pp. 143–154). Springer, Dordrecht. https://doi.org/10.1007/978-94-007-4001-3_255

16 Gajardo, G., & Redón, S. (2019). Andean hypersaline lakes in the Atacama Desert, northern Chile: Between lithium exploitation and unique biodiversity conservation. *Conservation Science and Practice*, *1*(9). https://doi.org/10.1111/csp2.94

17 Gao, Y., Jia, J., Lu, Y., Yang, T., Lyu, S., Shi, K., Zhou, F., & Yu, G. (2021). Determining dominating control mechanisms of inland water carbon cycling processes and associated gross primary productivity on regional and global scales. *Earth-Science Reviews 213*, 103497. https://doi.org/10.1016/j.earscirev.2020.103497

18 Garreaud, R., Vuille, M., & Clement, A. C. (2003). The climate of the Altiplano: Observed current conditions and mechanisms of past changes. *Palaeogeography, Palaeoclimatology, Palaeoecology*, *194*(1–3), 5–22. https://doi.org/10.1016/S0031-0182(03)00269-4

19 Halkes, R. T., Hughes, A., Wall, F., Petavratzi, E., Pell, R., & Lindsay, J. J. (2024). Life cycle assessment and water use impacts of lithium production from salar deposits: Challenges and opportunities. *Resources, Conservation, and Recycling*, *207*, 107554. https://doi.org/10.1016/j.resconrec.2024.107554

20 Hammer, U.T. (1981). Primary production in saline lakes: A review. In: Williams, W.D. (eds)

Salt Lakes. *Developments in Hydrobiology*, 5. Springer, Dordrecht. https://doi.org/10.1007/978-94-009-8665-7_5

21 Hernández, K. L., Yannicelli, B., Olsen, L. M., Dorador, C., Menschel, E. J., Molina, V., Remonsellez, F., Hengst, M. B., & Jeffrey, W. H. (2016). Microbial activity response to solar radiation across contrasting environmental conditions in Salar de Huasco, northern Chilean altiplano. *Frontiers in Microbiology*, *7*. https://doi.org/10.3389/fmicb.2016.01857

22 Huang, J., Yang, J., Han, M., Wang, B., Sun, X., & Jiang, H. (2023). Microbial carbon fixation and its influencing factors in saline lake water. *Science of the Total Environment*, *877*, 162922. https://doi.org/10.1016/j.scitotenv.2023.162922

23 Hull, V., Parrella, L., & Falcucci, M. (2008). Modelling dissolved oxygen dynamics in coastal lagoons. *Ecological Modelling*, *211*(3–4), 468–480. https://doi.org/10.1016/j.ecolmodel.2007.09.023

24 Jørgensen, S. E., & Bendoricchio, G. (2001). Chapter 3 Ecological processes. In S. E. Jørgensen & G. Bendoricchio (Eds.), Fundamentals of Ecological Modelling (Vol. 21, pp. 93–209). Elsevier. https://doi.org/https://doi.org/10.1016/S0167-8892(01)80005-1

25 Jørgensen, S. E., Nielsen, S. Nors., & Jørgensen, L. Albert. (1991). *Handbook of ecological parameters and ecotoxicology*. Elsevier.

26 Leppäranta, M. (2015). Thermodynamics of Seasonal Lake Ice. *Freezing of Lakes and the Evolution of their Ice Cover* (pp. 91–135). Springer Berlin Heidelberg. https://doi.org/10.1007/978-3-642-29081-7_4

27 Lobos-Roco, F., Hartogensis, O., Vilà-Guerau de Arellano, J., Aguirre, F., de La Fuente, A., & Suárez, F. (2022a). Optical-Microwave Scintillometer Evaporation measurements over a Saline Lake in a Heterogeneous Setting in the Atacama Desert. *Journal of Hydrometeorology*, *23*(6), 909-924 https://doi.org/10.1175/JHM-D-21-0100.1

28 Lobos-Roco, F., Hartogensis, O., Vilà-Guerau de Arellano, J, de la Fuente, A., Muñoz, R., Rutllant, J., & Suárez, F. (2021). Local evaporation controlled by regional atmospheric circulation in the Altiplano of the Atacama Desert. *Atmospheric Chemistry and Physics*, *21*(11), 9125–9150. https://doi.org/10.5194/acp-21-9125-2021

29 Lobos-Roco, F., Hartogensis, O., Suárez, F., Huerta-Viso, A., Benedict, I., de la Fuente, A., & Vilà-Guerau de Arellano, J. (2022b). Multi-scale temporal analysis of evaporation on a saline lake in the Atacama Desert. *Hydrology and Earth System Sciences*, *26*(13), 3709–3729. https://doi.org/10.5194/hess-26-3709-2022

30 Marazuela, M. A., Vázquez-Suñé, E., Ayora, C., García-Gil, A., & Palma, T. (2019). The effect of brine pumping on the natural hydrodynamics of the Salar de Atacama: The damping capacity of salt flats. *Science of the Total Environment*, *654*, 1118–1131. https://doi.org/10.1016/j.scitotenv.2018.11.196

31 Molina, V., Eissler, Y., Cornejo, M., Galand, P. E., Dorador, C., Hengst, M., Fernandez, C., & Francois, J. P. (2018). Distribution of greenhouse gases in hyper-arid and arid areas of

northern Chile and the contribution of the high altitude wetland microbiome (Salar de Huasco, Chile). *Antonie van Leeuwenhoek*, *111*(8), 1421–1432. https://doi.org/10.1007/s10482-018-1078-9

32 Molina, V., Eissler, Y., Fernandez, C., Cornejo-D'Ottone, M., Dorador, C., Bebout, B. M., Jeffrey, W. H., Romero, C., & Hengst, M. (2021). Greenhouse gases and biogeochemical diel fluctuations in a high-altitude wetland. *Science of the Total Environment*, *768*, 144370. https://doi.org/10.1016/j.scitotenv.2020.144370

33 Ordoñez, C., de la Fuente, A., & Díaz-Palma, P. (2015). Modeling the influence of benthic primary production on oxygen transport through the water-sediment interface. *Ecological Modelling*, *311*, 1–10. https://doi.org/10.1016/j.ecolmodel.2015.05.007

34 Paquis, P., Hengst, M. B., Florez, J. Z., Tapia, J., Molina, V., Pérez, V., & Pardo-Esté, C. (2023). Short-term characterisation of climatic-environmental variables and microbial community diversity in a high-altitude Andean wetland (Salar de Huasco, Chile). *Science of The Total Environment*, *859*, 160291. https://doi.org/https://doi.org/10.1016/j.scitotenv.2022.160291

35 Pardo-Esté, C., Leiva, S. G., Remonsellez, F., Castro-Nallar, E., Castro-Severyn, J., & Saavedra, C. P. (2023). Exploring the Influence of Small-Scale Geographical and Seasonal Variations Over the Microbial Diversity in a Poly-extreme Athalosaline Wetland. *Current Microbiology*, *80*, 297. https://doi.org/10.1007/s00284-023-03395-w

36 Richardson, J. L., Desai, A. R., Thom, J., Lindgren, K., Laudon, H., Peichl, M., Nilsson, M., Campeau, A., Järveoja, J., Hawman, P., Mishra, D. R., Smith, D., D'Acunha, B., Knox, S. H., Ng, D., Johnson, M. S., Blackstock, J., Malone, S. L., Oberbauer, S. F., … Matsumura, M. (2024). On the Relationship Between Aquatic CO_2 Concentration and Ecosystem Fluxes in Some of the World's Key Wetland Types. *Wetlands*, *44*, 1. https://doi.org/10.1007/s13157-023-01751-x

37 Sobol, I. M. (2001). Global sensitivity indices for nonlinear mathematical models and their Monte Carlo estimates. In *Mathematics and Computers in Simulation* (Vol. 55).

38 Stefan, H. G., & Fang, X. (1994). Dissolved oxygen model for regional lake analysis. *Ecological Modelling*, *71*(1-3), 37–68. https://doi.org/https://doi.org/10.1016/0304-3800(94)90075-2

39 Suárez, F., Lobos, F., de la Fuente, A., Vilà-Guerau de Arellano, J., Prieto, A., Meruane, C., & Hartogensis, O. (2020). E-DATA: A comprehensive field campaign to investigate evaporation enhanced by advection in the hyper-arid altiplano. *Water*, *12*(3), 745. https://doi.org/10.3390/w12030745

40 Tranvik, L. J., Downing, J. A., Cotner, J. B., Loiselle, S. A., Striegl, R. G., Ballatore, T. J., Dillon, P., Finlay, K., Fortino, K., Knoll, L. B., Kortelainen, P. L., Kutser, T., Larsen, S., Laurion, I., Leech, D. M., McCallister, S. L., McKnight, D. M., Melack, J. M., Overholt, E., … Weyhenmeyer, G. A. (2009). Lakes and reservoirs as regulators of carbon cycling and

climate. *Limnology and Oceanography*, *54*(6part2), 2298–2314. https://doi.org/10.4319/lo.2009.54.6_part_2.2298

41 Uribe Rivera, D., Vera Burgos, C., Paicho, M. & Espinoza, G. (2017). Observatorio ecosocial para el seguimiento del cambio climático en ecosistemas de altura en la región de Tarapacá: Propuestas, avances y proyecciones. *Diálogo Andino*, *54*, 63–82. https://doi.org/10.4067/S0719-26812017000300063

42 Wurtsbaugh, W. A., Miller, C., Null, S. E., DeRose, R. J., Wilcock, P., Hahnenberger, M., Howe, F., & Moore, J. (2017). Decline of the world's saline lakes. *Nature Geoscience*, *10*, 816–821. https://doi.org/10.1038/NGEO3052

43 Yue, L., Kong, W., Li, C., Zhu, G., Zhu, L., Makhalanyane, T. P., & Cowan, D. A. (2021). Dissolved inorganic carbon determines the abundance of microbial primary producers and primary production in Tibetan Plateau lakes. *FEMS Microbiology Ecology*, *97*(2). https://doi.org/10.1093/femsec/fiaa242

44 Zappa, C. J., McGillis, W. R., Raymond, P. A., Edson, J. B., Hintsa, E. J., Zemmelink, H. J., Dacey, J. W. H., & Ho, D. T. (2007). Environmental turbulent mixing controls on air-water gas exchange in marine and aquatic systems. *Geophysical Research Letters*, *34*(10). https://doi.org/10.1029/2006GL028790

Appendix

This part presents the details of the mathematical formulation of each process and flows.

A.1 Dissolved oxygen concentration

Specific processes involved in the $[O_2]$ mass balance are:

Net photosynthesis, $nPhS$: described in equation A.1, accounts for the contribution of the photosynthesis (PhS) minus photorespiration (PhR). For this process, the equations described in Hull et al. (2008) were used:

$$nPhS = PhS - PhR \tag{A.1}$$

The photosynthesis process is described as:

$$PhS = P_{max} \cdot f\left(Rsw_{eff}, [CO_2]_{aq}\right) \cdot Chla \tag{A.2}$$

where P_{max} is the maximum oxygen production due to photosynthesis, $f\left(Rsw_{eff}, [CO_2]_{aq}\right)$ is a limitation function of the effective solar radiation (Rsw_{eff}) and dissolved CO_2, and $Chla$ is the chlorophyll A concentration.

Equations A.3 and A.4 present the calculations for the maximum oxygen production P_{max} and for the function $f\left(Rsw_{eff}, [CO_2]_{aq}\right)$. For this last term a multiplicative limitation was

considered, i.e., it is defined as the product of the functions (Jørgensen & Bendoricchio, 2001):

$$P_{max} = \mu_{max} \cdot \theta_{PhS}^{(T_w - 20)} \quad \text{(A.3)}$$

$$f(Rsw_{eff}, [CO_2]_{aq}) = f(R_{sw,eff}) \cdot f([CO_2]_{aq}) = \frac{Rsw_{eff}}{Rsw_{eff} + \alpha_{Rad}} \cdot \frac{[CO_2]_{aq}}{[CO_2]_{aq} + k_{CO_2}} \quad \text{(A.4)}$$

where μ_{max} is the maximum oxygen production rate at 20°C, θ_{PhS} is the temperature correction coefficient, T_w is the water temperature, α_{Rsw} is the radiation half-saturation constant, and $k_{CO_2}$is the semi-saturation constant for carbon dioxide dissolved in water.

The effective radiation Rsw_{eff} depends on whether there is a layer of ice on the lake surface. For this, the equation described in Leppäranta (2015) is used:

$$Rsw_{eff} = (1 - \alpha) \cdot \Gamma \cdot Rsw \qquad \text{If there is ice cover} \quad \text{(A.5)}$$

$$Rsw_{eff} = Rsw \qquad \text{If not} \quad \text{(A.6)}$$

where, α is the albedo, and Γ is an empirical coefficient of the fraction of shear wave radiation crossing the ice surface, and Rsw is the measured incident radiation.
The photorespiration process is described as:

$$PhR = PR_{max} \cdot g(Rsw_{eff}, [O_2]_{aq}) \cdot Chla \quad \text{(A.7)}$$

where PR_{max} is the maximum photorespiration rate as a function of water temperature, $g(Rsw_{eff}, [O_2]_{aq})$ is the limitation function of the effective solar radiation Rsw_{eff} and $[O_2]_{aq}$, and $Chla$ is the chlorophyll A concentration.

Equations A.8 and A.9 present the calculations for the maximum photorespiration rate PR_{max} and for the limiting function $g(Rsw_{eff}, [O_2]_{aq})$. For this last term a multiplicative limitation was considered, i.e., it is defined as the product of the functions (Jørgensen & Bendoricchio, 2001):

$$PR_{max} = \alpha_{PhR} \cdot \theta_{PhR}^{(T_w - 20)} \quad \text{(A.8)}$$

$$g(Rsw_{eff}, [O_2]_{aq}) = g(Rsw_{eff}) \cdot g([O_2]_{aq}) = \frac{Rsw_{eff}}{Rsw_{eff} + \beta_{Rsw}} \cdot sin\left(\pi \frac{t}{24}\right)^{16} \cdot \left(\frac{[O_2]_{aq}}{[O_2]_{aq} + k_{O_2}}\right) \quad \text{(A.9)}$$

where α_{PhR} is the maximum oxygen consumption rate at 20°C, θ_{PhR} is a temperature correction coefficient, T_w is the water temperature, Rsw_{eff} is the effective solar radiation presented in equations A.5 and A.6, β_{Rsw} is the radiation half-saturation constant, t corresponds to the time of day, and k_{O_2} is the semi-saturation constant for oxygen dissolved in water.

Reaeration, $F_{O_2,AWI}$: described in equation A.10, corresponds to the exchange of oxygen between the atmosphere and the water body. For this process, the equation described in Hull et al. (2008) and Cole & Prairie (2009) were used:

$$F_{O_2,AWI} = k_{air,O_2} \cdot \left([O_{2,sat}]_{aq} - [O_2]_{aq}\right) \quad \text{(A.10)}$$

The following equation is used for the gas transfer velocity k_{air,O_2} (Zappa et al. (2007):

$$k_{air,O_2} = A_{O_2} \cdot (\varepsilon \cdot v)^{0,25} \cdot (Sc)^{-0,5} \quad \text{(A.11)}$$

Where, $\left[O_{2,sat}\right]_{aq}$ is the saturation concentration in water, A_{O_2} is a dimensionless constant, v corresponds to the kinematic viscosity of water, ε is the turbulent kinetic energy rate, and Sc is the Schmidt number.

Biological oxygen demand, BOD : described in equation A.12, denotes the microbial degradation of organic matter in water. For this process, the equations described in Hull et al. (2008) were used:

$$BOD = k_{BOD} \cdot \theta_{BOD}^{(T_w - 20)} \cdot DET \quad \text{(A.12)}$$

where, k_{BOD} is the organic matter degradation constant, θ_{BOD} is a temperature correction constant, T_w is the water temperature, and DET corresponds to the total detrital concentration, i.e., in the water column and in the sediments.

Respiration, Res : described in equation A.13, represents a model of respiration, a metabolic process carried out by photosynthetic organisms. For this process, the equations described in Hull et al. (2008) were used:

$$Res = \alpha_{Res} \cdot \theta_{Res}^{(T_w - 20)} \cdot Chla \quad \text{(A.13)}$$

where, α_{Res} is the respiration constant, T_w is the water temperature, and θ_{Res} is the temperature correction constant.

Oxygen exchange at the WSI, $F_{O_2,WSI}$: corresponds to a model of oxygen exchange at the water-sediment interface. For this process, the equations described in Ordoñez et al. (2015) were used.

The O_2 that is not consumed in the active sediment layer is called the effective oxygen dissolved production rate (P_{ef}):

$$P_{ef} = P - \overline{r_1} \cdot \delta_p \quad \text{(A.14)}$$

$$P = P_{max} \cdot f\left(Rsw_{eff,sed}, [CO_2]_{sed}\right) \cdot Chla_{sed} \quad \text{(A.15)}$$

where, $\overline{r_1}$ corresponds to the rate of consumption within the active layer, P is the rate of oxygen production in the sediments, P_{max} is the maximum oxygen production due to photosynthesis in sediments, δ_p corresponds to a thin layer on top of the sediments where benthic primary production occurs, $f\left(Rsw_{eff,sed}, [CO_2]_{sed}\right)$ is the limiting function relating the effective solar radiation on sediments $\left(Rsw_{eff,sed}\right)$ and CO_2 concentration in sediments, and $Chla_{sed}$ is the chlorophyll A concentration in sediments.

P_{max} and $f\left(Rsw_{eff,sed}, [CO_2]_{sed}\right)$ are described in equations A.17 and A.18. For this last term a multiplicative limitation was considered, i.e., it is defined as the product of the functions

(Jørgensen & Bendoricchio, 2001):

$$P_{max} = \mu_{max} \cdot \theta_{PhS}^{(T_w-20)} \quad \text{(A.16)}$$

$$f\left(Rsw_{eff,sed}, [CO_2]_{sed}\right) = f\left(Rsw_{eff,sed}\right) \cdot f([CO_2]_{sed})$$

$$f\left(Rsw_{eff,sed}, [CO_2]_{sed}\right) = \frac{1}{k_s \cdot \delta_p} \cdot ln\left(\frac{\alpha_{Rsw}+Rsw_{eff,sed}}{\alpha_{Rsw}}\right) \cdot \frac{[CO_2]_{sed}}{[CO_2]_{sed}+ k_{CO_2}} \quad \text{(A.17)}$$

where μ_{max} is the maximum oxygen production rate at 20°C, θ_{PhS} is the temperature correction coefficient, T_w is the water temperature, k_s is the attenuation coefficient of the active layer of algae, δ_p corresponds to a thin layer on top of the sediments where benthic primary production occurs, α_{Rsw} is the radiation half-saturation constant, and $k_{CO_2}$is the semi-saturation constant for carbon dioxide dissolved in water.

In the case of effective radiation in sediments, this varies due to the shading of algae and the sediments between them (De La Fuente, 2014):

$$Rsw_{eff,sed} = \alpha_{sed} \cdot Rsw_{eff} \cdot exp(-k_d \cdot h_w) \quad \text{(A.18)}$$

where, α_{sed} is a dimensionless constant, Rsw_{eff} is the effective solar radiation calculated with equations A.5 and A.6, k_d is the vertical attenuation coefficient, and h_w is the depth of the lagoon.

The equation to define the oxygen flux through WSI is calculated depending on the value of P_{ef}, if $P_{ef} \geq 0$, $F_{O_2,WSI}$ is obtained with equation A.20 (Ordoñez et al., 2015):

$$F_{O_2,WSI} = \frac{S_2}{2}\left[\left(\frac{1}{k_{WSI}} + 2\frac{P_a}{S_2}\right) - \sqrt{\left(\frac{1}{k_{WSI}} + 2\frac{P_a}{S_2}\right)^2 - 4\left(\frac{P_a P_{ef}}{{S_2}^2} - \frac{[O_2]_{aq}}{S_2} - (1-\alpha)\frac{\overline{r_2}\cdot\delta_p\cdot P}{{S_2}^2}\right)}\right] \quad \text{(A.19)}$$

$$S_2 = 2\phi\overline{r_2}D_s \quad \text{(A.20)}$$

$$P_a = P - \Delta\bar{r}\delta_p \quad \text{(A.21)}$$

$$\Delta\bar{r} = \overline{r_1} - \overline{r_2} \quad \text{(A.22)}$$

where, k_{WSI} is the diffusion mass transfer coefficient at the sediment-water interface (de la Fuente et al., 2016), D_s is the molecular diffusion coefficient modified by tortuosity, ϕ is the porosity of the upper layer sediment, $\overline{r_1}$ corresponds to the rate of consumption within the active layer, $\overline{r_2}$ is the rate of oxygen consumption below the active photosynthetic layer, and δ_p corresponds to a thin layer on top of the sediments.

On the contrary, if $P_{ef} < 0$, $F_{O_2,WSI}$ is calculated with equation A.24:

$$F_{O_2,WSI} = \frac{S_2}{2}\left[\left(\frac{1}{k_{WSI}} + 2\frac{2\Delta r_2\delta_p}{S_2}\right) - \sqrt{\left(\frac{1}{k_{WSI}} + 2\frac{2\Delta r_2\delta_p}{S_2}\right)^2 + 4\left(\frac{2\Delta r_2\delta_p}{{S_2}^2} + \frac{[O_2]_{aq}}{S_2}\right)}\right] \quad \text{(A.23)}$$

$$\Delta\overline{r_2} = \overline{r_3} - \overline{r_2} \quad \text{(A.24)}$$

$$\overline{r_3} = \overline{r_1} - \frac{\alpha_p P}{\delta_p} \quad \text{(A.25)}$$

where, α_p represents the variability of the rate of DO production.

However, it must be determined which consumption rate is influencing the flow value. In the case where $\frac{F_{O_2,WSI}}{\overline{r_3}} \geq \delta_p$, the flow is influenced by the area under δ_p and equation A.24 is representative of the problem, on the contrary, if $\frac{F_{O_2,WSI}}{\overline{r_3}} < \delta_p$, the flow is only influenced by $\overline{r_1}$ and the equation to calculate it is:

$$F_{O_2,WSI} = \frac{S_3}{2}\left[\left(\frac{1}{k_{WSI}}\right) - \sqrt{\left(\frac{1}{k_{WSI}}\right)^2 - 4\left(\frac{[O_2]_{aq}}{S_3}\right)}\right] \quad \text{(A.26)}$$

$$S_3 = 2\phi\overline{r_3}D_s \quad \text{(A.27)}$$

$$\overline{r_3} = \overline{r_1} - \frac{\alpha_p \cdot P}{\delta_p} \quad \text{(A.28)}$$

where, $\overline{r_1}$ corresponds to the rate of consumption within the active layer δ_p, α_p represents the variability of the rate of dissolved O_2 production, k_{WSI} is the diffusion mass transfer coefficient, D_s is the molecular diffusion coefficient modified by tortuosity, and ϕ is the porosity of the upper layer sediment.

A.2 Dissolved carbon dioxide concentration

Specific processes involved in the $[CO_2]$ mass balance are:

Net photosynthesis, $\boldsymbol{nPhS}$**:** the details of this process are presented in equations A.1 to A.9.

Respiration, Res : the details of this process are presented in equation A.13.

Carbon dioxide exchange at the AWI, $F_{CO_2,AWI}$: described in equation A.29, corresponds to a model of CO_2 exchange between the aqueous and gas phases. For this process, the equations described in Hull et al. (2008) were used:

$$F_{CO_2,AWI} = k_{air,CO_2} \cdot \left(\left[CO_{2,sat}\right]_{aq} - [CO_2]_{aq}\right) \quad \text{(A.29)}$$

The following equation is used for the gas transfer velocity k_{air,CO_2} (Zappa et al. (2007):

$$k_{air,CO_2} = A_{CO_2} \cdot (\varepsilon \cdot v)^{0,25} \cdot (Sc)^{-0,5} \quad \text{(A.30)}$$

where $k_{air,CO_2}$is the gas transfer velocity, $\left[CO_{2,sat}\right]_{aq}$is the saturation concentration in water, A_{CO_2} is a dimensionless constant, v corresponds to the kinematic viscosity of water, ε is the turbulent kinetic energy rate, and Sc is the Schmidt number.

Carbon dioxide exchange at the WSI, $F_{CO_2,WSI}$: described in equation A.31, corresponds to a model of CO_2 exchange at the water-sediment interface.

$$F_{CO_2,WSI} = \frac{S_{CO_2}}{2 \cdot k_{WSI}} \cdot \left(1 - \sqrt{1 + 4 \cdot \left(\frac{k_{WSI}^2 \cdot [CO_2]_{aq}}{S_{CO_2}}\right)}\right) \quad \text{(A.31)}$$

$$S_{CO_2} = 2\phi \cdot \bar{r}_{CO_2} \cdot D_s \quad \text{(A.32)}$$

$$\bar{r}_{CO_2} = P \cdot k_{O_2-CO_2} \quad \text{(A.33)}$$

where, k_{WSI} is the diffusion mass transfer coefficient at the sediment-water interface, D_s is the molecular diffusion coefficient modified by tortuosity, ϕ is the porosity of the upper layer sediment, $\bar{r}_{CO_2}$ is the consumption rate due to photosynthesis, P is the sediment oxygen production described in equation A.15, and $k_{O_2-CO_2}$ is the constant relating the rates at which CO_2 consumption occurs as a function of O_2 production due to photosynthesis.

A.3 Biomass concentration

For these processes, the equations described in Hull et al. (2008) are considered as a basis, but some modifications were made. For biomass $[B]$, a balance between growth ($Grow$) and biomass loss ($Loss$) is performed. Because this variable is present in both the water column and sediments, the balance is described by the following processes:

Growth of biomass in water, $Grow_{wat}$: described in equation A.34, corresponds to the growth of biomass associated with primary producers within the water column.

$$Grow_{wat} = nPhS \cdot k_{C-O_2} \quad \text{(A.34)}$$

where, $nPhS$ corresponds to net photosynthesis and k_{C-O_2} is the stoichiometric constant between carbon and oxygen.

Growth of biomass in sediments, $Grow_{sed}$: described in equation A.35, corresponds to the growth of biomass associated with primary producers in the sediments. For this process, the equations described in Hull et al. (2008) were used:

$$Grow_{sed} = P \cdot k_{C-O_2} \quad \text{(A.35)}$$

where, P is the production in sediments calculated with equation A.15 and k_{C-O_2} is the stoichiometric constant between carbon and oxygen.

Loss of biomass in water, $Loss_{wat}$: described in equation A.36, corresponds to the loss of biomass in the water column.

$$Loss_{wat} = k_{dead} \cdot B_{wat} \quad \text{(A.36)}$$

$$B_{wat} = B \cdot SST \quad \text{(A.37)}$$

where, k_{dead} is the biomass death rate, B_{wat} is the biomass concentration in the water column, and SST corresponds to the fraction of sediment that resuspends from the sediments.

Loss of biomass in sediments, $Loss_{sed}$: described in equation 3.8, corresponds to the loss of biomass in the sediments.

$$Loss_{sed} = k_{dead} \cdot B_{sed} \tag{A.38}$$

$$B_{sed} = B \cdot (1 - SST) \tag{A.39}$$

where, k_{dead} is the biomass death rate, B_{sed} is the biomass concentration in the sediments, and SST corresponds to the fraction of sediment that resuspends.

A.4 Detritus concentration

For these processes, the equations described in Hull et al. (2008) are considered as a basis, but some modifications were made. For the mass balance of detritus, it is considered that the production of dead biomass increases the amount of substrate, while the degradation of organic matter consumes the substrate. Specific processes involved in the $[DET]$ mass balance are:

Loss of biomass in water, $Loss_{wat}$: corresponds to the loss of biomass in the water column. The details are presented in equations A.36 and A.37.

Loss of biomass in sediments, $Loss_{sed}$: corresponds to the loss of biomass in the sediments. The details are presented in equations A.38 and A.39.

Biological oxygen demand, BOD : denotes the microbial degradation of organic matter in water. The details are presented in equation A.12.

Oxygen consumption in sediments, $\bar{r}$: presented in equation A.14, corresponds to the rate of consumption within the active layer δ_p.

III. Conclusiones

Los salares son hábitats con una reserva única de biodiversidad y desempeñan un papel clave en los ciclos de los gases de efecto invernadero. Estos sistemas tienen una dinámica cerrada, lo que significa que cualquier cambio, por pequeño que parezca, genera efectos que pueden desequilibrar los ciclos físicos, químicos y biológicos.

Los lagos salinos presentan interacciones atmósfera-superficie que varían en diferentes escalas temporales y desencadenan cambios en los ciclos bioquímicos. En este trabajo estudiamos los efectos del forzamiento meteorológico sobre los diferentes procesos que se llevan a cabo en estos sistemas acuáticos. Se desarrolló un modelo 0-D transitorio capaz de simular las concentraciones de O_2 y CO_2 en una laguna somera presente en el Salar del Huasco. Esto con el fin de estudiar la influencia de los factores ambientales en la dinámica de los procesos bioquímicos y de transporte y, por lo tanto, en la calidad de agua del sistema. Los resultados indican que los factores meteorológicos tienen efectos significativos sobre los humedales altoandinos. En particular, se concluye que una de las principales forzantes externas es la velocidad del viento y que un cambio en esta variable puede generar mayores impactos que las fluctuaciones en la

temperatura. Por esta razón, es relevante considerar el régimen de viento en los estudios de cambio climático, especialmente cuando se realizan análisis a escala intradiaria.

Por otra parte, sería interesante incorporar en futuras versiones del modelo otros procesos relacionados con las variables de estudio, como reacciones asociadas al sistema carbonato y procesos anaeróbicos. Además, como se ha mencionado anteriormente, los salares juegan un papel esencial en el cambio climático, por lo que se podrían incorporar otras variables de control asociadas a los gases de efecto invernadero (por ejemplo, metano y óxido nitroso) y analizar el comportamiento de la laguna. Sumado a esto, se recomienda realizar campañas de terreno más detalladas en diferentes estaciones del año para disponer de mediciones continuas de todas las variables de control. Por ejemplo, contar con datos de concentración de CO_2 en la columna de agua permitiría una mejor calibración y así lograr simulaciones más precisas de cada proceso que se lleva a cabo en el Salar del Huasco.

El modelo presentado en este estudio corresponde a una primera aproximación del funcionamiento de este tipo de sistema acuático. Es importante señalar que la metodología presentada es transferible para simular procesos en lagunas de otras partes del mundo que cuenten con la información meteorológica y de calidad de agua necesaria.

IV. Bibliografía

1 Aguirre-Correa, F., de Arellano, J. V. G., Ronda, R., Lobos-Roco, F., Suárez, F., & Hartogensis, O. (2023). Midday Boundary-Layer Collapse in the Altiplano Desert: The Combined Effect of Advection and Subsidence. *Boundary-Layer Meteorology*, *187*(3), 643-671. https://doi.org/10.1007/s10546-023-00790-5

2 Burkhardt, S., Amoroso, G., Riebesell, U., & Sültemeyer, D. (2001). CO_2 and HCO_3^- uptake in marine diatoms acclimated to different CO_2 concentrations. *Limnology and Oceanography*, *46*(6), 1378–1391. https://doi.org/10.4319/lo.2001.46.6.1378

3 Caziani, S. M., Rocha Olivio, O., Rodríguez Ramírez, E., Romano, M., Derlindati, E. J., Tálamo, A., Ricalde, D., Quiroga, C., Pablo Contreras, J., Valqui, M., & Sosa, H. (2007). Seasonal distribution, abundance, and nesting of Puna, Andean, and Chilean Flamingos. *The Condor*, *109*(2), 276–287. https://doi.org/10.1093/condor/109.2.276

4 CEAZA (n. d.). Red de estaciones meteorológicas: CEAZA-Met, Chile. https://www.ceazamet.cl/index.php?pag=mod_mapa&p_cod=ceazamet

5 Chapra, S. C., & Canale, R. P. (2015). *Numerical methods for engineers*. McGraw-Hill Education.

6 Cole, J. J., & Prairie, Y. T. (2009). Dissolved CO_2. In G. E. Likens (Ed.), *Encyclopedia of Inland Waters* (pp. 30–34). Academic Press. https://doi.org/https://doi.org/10.1016/B978-012370626-3.00091-0

7 Decreto No. 66, Crea Parque Nacional Salar del Huasco, en la Región de Tarapacá, y deja sin efecto los decretos N° 24 de 2019 y N° 5 de 2022, no tramitados, Marzo 1, 2023, Diario Oficial [D.O.] (Chile). https://www.diariooficial.interior.gob.cl/publicaciones/2023/03/01/43490/01/2279009.pdf

8 de la Fuente, A. (2014). Heat and dissolved oxygen exchanges between the sediment and water column in a shallow salty lagoon. *Journal of Geophysical Research: Biogeosciences*, *119*(4), 596–613. https://doi.org/10.1002/2013JG002413

9 de la Fuente, A., & Meruane, C. (2017). Spectral model for long-term computation of thermodynamics and potential evaporation in shallow wetlands. *Water Resources Research*, *53*(9), 7696–7715. https://doi.org/10.1002/2017WR020515

10 de la Fuente, A., Meruane, C., & Suárez, F. (2021). Long-term spatiotemporal variability in high Andean wetlands in northern Chile. *Science of the Total Environment*, *756*. https://doi.org/10.1016/j.scitotenv.2020.143830

11 de la Fuente, A., & Niño, Y. (2010). Temporal and spatial features of the thermohydrodynamics of shallow salty lagoons in northern Chile. *Limnology and Oceanography*, *55*(1), 279–288. https://doi.org/10.4319/lo.2010.55.1.0279

12 De los Rios-Escalante, P. R., Esse, C., Correa-Araneda, F., Rodríguez, L., Fernandez, C.E.,

Prado, P.E. (2024). Potential Effects of Climate Change in Saline Shallow Lakes in the North of Chile (Salar de Atacama, 23°S, Chile) and South Lipez of Bolivia (Khalina Lake, 22.61°S). In: Singh, A.L., Jamal, S., Ahmad, W.S. (eds) *Climate Change, Vulnerabilities and Adaptation: Understanding and Addressing Threats with Insights for Policy and Practice* (pp. 171–182). Springer Nature Switzerland. https://doi.org/10.1007/978-3-031-49642-4_9

13 Dorador, C., Molina, V., Hengst, M., Eissler, Y., Cornejo, M., Fernández, C., & Pérez, V. (2020). Microbial Communities Composition, Activity, and Dynamics at Salar de Huasco: A Polyextreme Environment in the Chilean Altiplano. In M. E. Farías (Ed.), *Microbial Ecosystems in Central Andes Extreme Environments: Biofilms, Microbial Mats, Microbialites and Endoevaporites* (pp. 123–139). Springer International Publishing. https://doi.org/10.1007/978-3-030-36192-1_9

14 Downing, J. A., Prairie, Y. T., Cole, J. J., Duarte, C. M., Tranvik, L. J., Striegl, R. G., McDowell, W. H., Kortelainen, P., Caraco, N. F., Melack, J. M., & Middelburg, J. J. (2006). The global abundance and size distribution of lakes, ponds, and impoundments. *Limnology and Oceanography*, *51*(5), 2388–2397. https://doi.org/10.4319/lo.2006.51.5.2388

15 Finlayson, C.M. (2018). Salt Lakes. In: Finlayson, C., Milton, G., Prentice, R., Davidson, N. (eds). The Wetland Book: II: Distribution, Description, and Conservation. (pp. 143–154). Springer, Dordrecht. https://doi.org/10.1007/978-94-007-4001-3_255

16 Gajardo, G., & Redón, S. (2019). Andean hypersaline lakes in the Atacama Desert, northern Chile: Between lithium exploitation and unique biodiversity conservation. *Conservation Science and Practice*, *1*(9). https://doi.org/10.1111/csp2.94

17 Gao, Y., Jia, J., Lu, Y., Yang, T., Lyu, S., Shi, K., Zhou, F., & Yu, G. (2021). Determining dominating control mechanisms of inland water carbon cycling processes and associated gross primary productivity on regional and global scales. *Earth-Science Reviews 213*, 103497. https://doi.org/10.1016/j.earscirev.2020.103497

18 Garreaud, R., Vuille, M., & Clement, A. C. (2003). The climate of the Altiplano: Observed current conditions and mechanisms of past changes. *Palaeogeography, Palaeoclimatology, Palaeoecology*, *194*(1–3), 5–22. https://doi.org/10.1016/S0031-0182(03)00269-4

19 Halkes, R. T., Hughes, A., Wall, F., Petavratzi, E., Pell, R., & Lindsay, J. J. (2024). Life cycle assessment and water use impacts of lithium production from salar deposits: Challenges and opportunities. *Resources, Conservation, and Recycling*, *207*, 107554. https://doi.org/10.1016/j.resconrec.2024.107554

20 Hammer, U.T. (1981). Primary production in saline lakes: A review. In: Williams, W.D. (eds) Salt Lakes. *Developments in Hydrobiology*, 5. Springer, Dordrecht. https://doi.org/10.1007/978-94-009-8665-7_5

21 Hernández, K. L., Yannicelli, B., Olsen, L. M., Dorador, C., Menschel, E. J., Molina, V., Remonsellez, F., Hengst, M. B., & Jeffrey, W. H. (2016). Microbial activity response to solar radiation across contrasting environmental conditions in Salar de Huasco, northern Chilean altiplano. *Frontiers in Microbiology*, *7*. https://doi.org/10.3389/fmicb.2016.01857

22 Hidalgo, F. (2017). Caracterización y cuantifiación de los procesos de transporte-reacción que dominan la dinámica intradiaria de dióxido de carbono y oxígeno en el Salar del Huasco. Santiago, Facultad de Ciencias Físicas y Matemáticas, Universidad de Chile. https://repositorio.uchile.cl/handle/2250/150693

23 Huang, J., Yang, J., Han, M., Wang, B., Sun, X., & Jiang, H. (2023). Microbial carbon fixation and its influencing factors in saline lake water. *Science of the Total Environment*, *877*, 162922. https://doi.org/10.1016/j.scitotenv.2023.162922

24 Hull, V., Parrella, L., & Falcucci, M. (2008). Modelling dissolved oxygen dynamics in coastal lagoons. *Ecological Modelling*, *211*(3–4), 468–480. https://doi.org/10.1016/j.ecolmodel.2007.09.023

25 Jørgensen, S. E., & Bendoricchio, G. (2001). Chapter 3 Ecological processes. In S. E. Jørgensen & G. Bendoricchio (Eds.), Fundamentals of Ecological Modelling (Vol. 21, pp. 93–209). Elsevier. https://doi.org/https://doi.org/10.1016/S0167-8892(01)80005-1

26 Jørgensen, S. E., Nielsen, S. Nors., & Jørgensen, L. Albert. (1991). *Handbook of ecological parameters and ecotoxicology*. Elsevier.

27 Leppäranta, M. (2015). Thermodynamics of Seasonal Lake Ice. *Freezing of Lakes and the Evolution of their Ice Cover* (pp. 91–135). Springer Berlin Heidelberg. https://doi.org/10.1007/978-3-642-29081-7_4

28 Lobos-Roco, F., Hartogensis, O., Vilà-Guerau de Arellano, J., Aguirre, F., de La Fuente, A., & Suárez, F. (2022a). Optical-Microwave Scintillometer Evaporation measurements over a Saline Lake in a Heterogeneous Setting in the Atacama Desert. *Journal of Hydrometeorology*, *23*(6), 909-924 https://doi.org/10.1175/JHM-D-21-0100.1

29 Lobos-Roco, F., Hartogensis, O., Vilà-Guerau de Arellano, J, de la Fuente, A., Muñoz, R., Rutllant, J., & Suárez, F. (2021). Local evaporation controlled by regional atmospheric circulation in the Altiplano of the Atacama Desert. *Atmospheric Chemistry and Physics*, *21*(11), 9125–9150. https://doi.org/10.5194/acp-21-9125-2021

30 Lobos-Roco, F., Hartogensis, O., Suárez, F., Huerta-Viso, A., Benedict, I., de la Fuente, A., & Vilà-Guerau de Arellano, J. (2022b). Multi-scale temporal analysis of evaporation on a saline lake in the Atacama Desert. *Hydrology and Earth System Sciences*, *26*(13), 3709–3729. https://doi.org/10.5194/hess-26-3709-2022

31 Marazuela, M. A., Vázquez-Suñé, E., Ayora, C., García-Gil, A., & Palma, T. (2019). The effect of brine pumping on the natural hydrodynamics of the Salar de Atacama: The damping capacity of salt flats. *Science of the Total Environment*, *654*, 1118–1131. https://doi.org/10.1016/j.scitotenv.2018.11.196

32 Molina, V., Eissler, Y., Cornejo, M., Galand, P. E., Dorador, C., Hengst, M., Fernandez, C., & Francois, J. P. (2018). Distribution of greenhouse gases in hyper-arid and arid areas of northern Chile and the contribution of the high altitude wetland microbiome (Salar de Huasco, Chile). *Antonie van Leeuwenhoek*, *111*(8), 1421–1432. https://doi.org/10.1007/s10482-018-

1078-9

33 Molina, V., Eissler, Y., Fernandez, C., Cornejo-D'Ottone, M., Dorador, C., Bebout, B. M., Jeffrey, W. H., Romero, C., & Hengst, M. (2021). Greenhouse gases and biogeochemical diel fluctuations in a high-altitude wetland. *Science of the Total Environment*, *768*, 144370. https://doi.org/10.1016/j.scitotenv.2020.144370

34 Ordoñez, C., de la Fuente, A., & Díaz-Palma, P. (2015). Modeling the influence of benthic primary production on oxygen transport through the water-sediment interface. *Ecological Modelling*, *311*, 1–10. https://doi.org/10.1016/j.ecolmodel.2015.05.007

35 Paquis, P., Hengst, M. B., Florez, J. Z., Tapia, J., Molina, V., Pérez, V., & Pardo-Esté, C. (2023). Short-term characterisation of climatic-environmental variables and microbial community diversity in a high-altitude Andean wetland (Salar de Huasco, Chile). *Science of The Total Environment*, *859*, 160291. https://doi.org/https://doi.org/10.1016/j.scitotenv.2022.160291

36 Pardo-Esté, C., Leiva, S. G., Remonsellez, F., Castro-Nallar, E., Castro-Severyn, J., & Saavedra, C. P. (2023). Exploring the Influence of Small-Scale Geographical and Seasonal Variations Over the Microbial Diversity in a Poly-extreme Athalosaline Wetland. *Current Microbiology*, *80*, 297. https://doi.org/10.1007/s00284-023-03395-w

37 Richardson, J. L., Desai, A. R., Thom, J., Lindgren, K., Laudon, H., Peichl, M., Nilsson, M., Campeau, A., Järveoja, J., Hawman, P., Mishra, D. R., Smith, D., D'Acunha, B., Knox, S. H., Ng, D., Johnson, M. S., Blackstock, J., Malone, S. L., Oberbauer, S. F., … Matsumura, M. (2024). On the Relationship Between Aquatic CO_2 Concentration and Ecosystem Fluxes in Some of the World's Key Wetland Types. *Wetlands*, *44*, 1. https://doi.org/10.1007/s13157-023-01751-x

38 Sobol, I. M. (2001). Global sensitivity indices for nonlinear mathematical models and their Monte Carlo estimates. In *Mathematics and Computers in Simulation* (Vol. 55).

39 Stefan, H. G., & Fang, X. (1994). Dissolved oxygen model for regional lake analysis. *Ecological Modelling*, *71*(1-3), 37–68. https://doi.org/https://doi.org/10.1016/0304-3800(94)90075-2

40 Suárez, F., Lobos, F., de la Fuente, A., Vilà-Guerau de Arellano, J., Prieto, A., Meruane, C., & Hartogensis, O. (2020). E-DATA: A comprehensive field campaign to investigate evaporation enhanced by advection in the hyper-arid altiplano. *Water*, *12*(3), 745. https://doi.org/10.3390/w12030745

41 Tranvik, L. J., Downing, J. A., Cotner, J. B., Loiselle, S. A., Striegl, R. G., Ballatore, T. J., Dillon, P., Finlay, K., Fortino, K., Knoll, L. B., Kortelainen, P. L., Kutser, T., Larsen, S., Laurion, I., Leech, D. M., McCallister, S. L., McKnight, D. M., Melack, J. M., Overholt, E., … Weyhenmeyer, G. A. (2009). Lakes and reservoirs as regulators of carbon cycling and climate. *Limnology and Oceanography*, *54*(6part2), 2298–2314. https://doi.org/10.4319/lo.2009.54.6_part_2.2298

42 Uribe Rivera, D., Vera Burgos, C., Paicho, M. & Espinoza, G. (2017). Observatorio ecosocial para el seguimiento del cambio climático en ecosistemas de altura en la región de Tarapacá: Propuestas, avances y proyecciones. *Diálogo Andino*, *54*, 63–82. https://doi.org/10.4067/S0719-26812017000300063

43 Vera, G. (2021). Caracterización y modelamiento fisicoquímico del transporte y reactividad de dióxido de carbono en el Salar de Huasco. Santiago, Facultad de Ciencias Físicas y Matemáticas, Universidad de Chile. https://repositorio.uchile.cl/handle/2250/183017

44 Wurtsbaugh, W. A., Miller, C., Null, S. E., DeRose, R. J., Wilcock, P., Hahnenberger, M., Howe, F., & Moore, J. (2017). Decline of the world's saline lakes. *Nature Geoscience*, *10*, 816–821. https://doi.org/10.1038/NGEO3052

45 Yue, L., Kong, W., Li, C., Zhu, G., Zhu, L., Makhalanyane, T. P., & Cowan, D. A. (2021). Dissolved inorganic carbon determines the abundance of microbial primary producers and primary production in Tibetan Plateau lakes. *FEMS Microbiology Ecology*, *97*(2). https://doi.org/10.1093/femsec/fiaa242

46 Zappa, C. J., McGillis, W. R., Raymond, P. A., Edson, J. B., Hintsa, E. J., Zemmelink, H. J., Dacey, J. W. H., & Ho, D. T. (2007). Environmental turbulent mixing controls on air-water gas exchange in marine and aquatic systems. *Geophysical Research Letters*, *34*(10). https://doi.org/10.1029/2006GL028790